Depositional environment and sequence stratigraphy of the Qom Formation (Miocene) from the Ghalibaf section, Central Iran

Ambiente deposicional y estratigrafía secuencial de la Formación Qom (Mioceno) de la sección Ghalifab, Irán Central

Jafar **Sharifi**[1], Yaghub **Nasiri**[2,*], Mahdi **Badpa**[3], Samira **Taghdisi Nikbakht**[2], Suman **Sarkar**[4], Mehdi **Hadi**[5]

[1] Department of Geology, Payame Noor University, Tehran, Iran.

[2] Geology Department, Faculty of Science, University of Gonabad, Gonabad, Iran.

[3] Independent researcher, Graduated from Stratigraphy and paleontology, Tehran, Iran.

[4] Birbal Sahni Institute of Palaeosciences, Lucknow - 226007, India.

[5] Independent researcher, Graduated from Stratigraphy and paleontology, Mashhad, Iran.

* Corresponding author: (Y. Nasiri)
y.nasiri.1365@gmail.com

How to cite this article:
Sharifi, J., Nasiri, Y., Badpa, M., Taghdisi Nikbakht, S., Sarkar, S., Hadi, M., 2023, Depositional environment and sequence stratigraphy of the Qom Formation (Miocene) from the Ghalibaf section, Central Iran: Boletín de la Sociedad Geológica Mexicana, 75 (3), A061023. http://dx.doi.org/10.18268/BSGM2023v75n3a061023

Manuscript received: April 25, 2023.
Corrected manuscript received: September 22, 2023.
Manuscript accepted: October 3, 2023.

Peer Reviewing under the responsibility of Universidad Nacional Autónoma de México.

ABSTRACT

The Miocene strata of the Qom Formation from the Ghalibaf section, Central Iran (NW Semnan) documented a high diversity of shallow-marine microfacies. These deposits in the Ghalibaf section, with a total thickness of 445 m, are characterized by twenty-one microfacies. The carbonate microfacies are deposited into five facies belts, including a lagoon, upper slope, lower slope, platform-margin sand shoals and margin facies. The presence of barrier reefs, intraclasts, oncoids, and grainstone aggregates, along with the absence of vast tidal flat areas, are distinguished. According to the aforementioned evidences, these sediments were deposited on a rimmed carbonate platform. In addition, the heterolithic calciturbidite deposits also show that the carbonate sequences were sedimented on a rimmed carbonate platform. Based on the available data of sequence stratigraphy analysis, seven third-order depositional sequences are bounded by type-1 and type-2 sequence boundaries. The relative sea-level changes between the upper and lower sequence boundaries in accord with the global sea-level curves reveal a reasonable correlation. However, some differences in other sequence boundaries might be due to local tectonic activities in the Qom Formation sedimentary basin, thereby leading to local sea-level changes. Moreover, biostratigraphic data based on the larger foraminifera index markers, including *Praebullalveolina curdica*, *Borelis melo*, *Dendritina rangi*, *Meandropsina iranica*, *Elphidium* sp. 14, *Neorotalia viennoti*, and *Miogypsina* sp. suggests the Miocene Shallow Benthic Zones, SBZ24-SBZ25 equivalent to the late Aquitanian-Burdigalian timespan.

Keywords: Qom Formation, Miocene, Sequence Stratigraphy, Central Iran, Microfacies.

RESUMEN

Los estratos del Mioceno de la Formación Qom Formation en la sección Ghalibaf, Irán Central (NO Semnan), documentan una alta diversidad de microfacies marinas someras. Estos depósitos, en la sección Ghalibaf, con un espesor total de 445 m, se caracterizan por veitiún microfacies. Las microfacies de carbonatosfueron depositadas en cinco cinturones de facies, incluyendo laguna, pendiente superior, pendiente inferior, bancos de arena de margen de plataforma y facies marginales en una plataforma carbonatada bordeada. La presencia de barreras de arrecifes, intraclastos, oncoides, The presence of barrier reefs, intraclasts, oncoids, y calizas granulares de carga agregada, junto con la ausencia de vastas areas de planicie de mareas, logran distinguirse. De acuerdo a las evidencias antes mencionadas, estos sedimentos fueron depositados en una plataforma carbonatada marginada. Adicionalmente, el carácter heterolítico de depósitos de calcirrudita muestran que las secuencias fueron despositadas en el tipo de plataforma citado. Con base en los datos disponibles de análisis de estratigrafía secuencial, setentaytres órdenes de secuencias deposicionales se caracterizan por límites de secuencia topoe-1 y tipo. Los cambios de nivel del mar relativos entre los límites de secuencia superior e inferior, de acuerdo a las curvas del nivel global del mar, revelan una correlación razonable. Sin embargo, algunas diferencias en otros límites de secuencia pueden deberse a actividad tectónica local en la cuenca sedimentaria de la Formación Qom, lo que produciría cambios locales del nivel del mar. Adicionalmente, datos bioestratigráficos basados en grandes foraminíferos, marcadores índice, que incluyen Praebullalveolina curdica, Borelis melo, Dendritina rangi, Meandropsina iranica, Elphidium sp. 14, Neorotalia viennoti y Miogypsina sp., sugieren las Zonas Bénticas Someras del Mioceno SBZ24-SBZ25, las cuales son equivalentes al lapso temporal del Aquitanian tardío-Burdigalian.

Palabras clave: Formación Qom; Mioceno; Estratigrafía secuencial; Irán Central; Microfacies.

http://dx.doi.org/10.18268/BSGM2023v75n3a061023

1. Introduction

The Qom Formation (the main hydrocarbon reservoir) is a thick carbonate succession of the Oligocene–Miocene in the central Iran region (*e.g.*, James and Wynd, 1965; Stöcklin and Setudehnia, 1991). This formation also outcrops in many localities in the Sanandaj-Sirjan Zone, and Uromia-Dokhtar Magmatic Arc, where these sediments are known as series of carbonate and mixed siliciclastic-carbonate deposits (*e.g.*, Stöcklin and Setudehnia, 1991; Agard *et al.*, 2005). The Oligo-Miocene shallow marine carbonates often contain diverse assemblages of benthic foraminifera that have been extensively used in different aspects such as biostratigraphy, palaeoenvironmental interpretation, and palaeobiogeography from the Western Tethys, the Middle East, and the Indo-Pacifc regions (*e.g.*, Henson, 1948; Bozorgnia, 1965; Vaziri-Moghaddam *et al.*, 2006; Hottinger, 2007; Boukhary *et al.*, 2010; Özcan *et al.*, 2010; Saraswati *et al.*, 2018; Hadi *et al.*, 2023).

Central Iran is surrounded by the Palaeo-Tethys suture zone towards the north and the Neo-Tethys towards the south (Aghanabati, 2006). The last marine transgression in Central Iran is recorded during the Rupelian–Burdigalian stages (Aghanabati, 2006). Berberian (2005) believed that the Qom sedimentary basin was created by subduction of the Neo-Tethyan oceanic plate beneath the Iranian platform. However, Morley *et al.* (2009) suggested that this sedimentary basin was constituted by the subsidence of Central Iran plate. They also proposed that the crust of central Iran was uplifted by Eocene volcanic activity. Subsequently, during the Late Oligocene-Early Miocene, subsidence occurred in central Iran under the cooling of the mantle (see Morley *et al.*, 2009). Furthermore, Reuter *et al.* (2009) noted that the deposits in the Qom sedimentary basin indicate transgressive conditions during the late Early Oligocene and Late Oligocene. Based on the position of the Iranian platform and widespread deposition of the Qom Formation, these outcrops can play a key role in the reconstruction of the bridge between the eastern Tethys (the proto-Indian Ocean) and the western Tethys (the proto-Mediterranean Sea) regions (Reuter *et al.*, 2009; Mohammadi *et al.*, 2015; Yazdi-Moghadam *et al.*, 2018a). Taking into account the available records from the Qom deposits by many authors (*e.g.* Reuter *et al.*, 2009; Mohammadi *et al.*, 2015; Yazdi-Moghadam *et al.*, 2018a, 2021), these show greater attention on the biostratigraphic data. Therefore, we elaborate a depositional model for the Miocene deposits of the Qom Formation from the Ghalibaf section with focus on the different approaches such as 1) the analysis of the sedimentary facies and the depositional setting, 2) presenting the variations in the depositional and palaeoenvironmental backgrounds, 3) biostratigraphic descriptions to identify the index faunal assemblages of the paleoenvironment and, 4) sequence stratigraphic framework of the Qom Formation.

2. Geological Setting and stratigraphy

The Iranian plateau is part of the Alpine-Himalayan system mountain belt and has been subdivided into eight sedimentary-structural provinces, each one characterized by some unique tectonic and sedimentary events (Stöcklin, 1968, Figure 1a): (1) Alborz, (2) Central Iran, (3) Zagros, (4) Kopet Dagh, (5) Eastern Iran, (6) Sanandaj-Sirjan, (7) Urumieh- Dokhtar (Sahand-Bazman) magmatic arc, and (8) Makran. The Qom Formation is present in the Sanandaj–Sirjan fore-arc and Central Iran back-arc basins (Figure1b). The first marine transgression of the Qom Sea can be traced back to the Early Oligocene in the fore-arc basin and to the Late Oligocene in the back-arc basin (Reuter *et al.*, 2007). These basins are separated by a volcanic arc system which formed during the Eocene (*e.g.* Stocklin and Setudehnia, 1991).

The central Iran basin displays complicated structural characteristics that are the result of many events in geological history from the Palaeozoic time up to the Present (Stocklin and Setudehnia,

http://dx.doi.org/10.18268/BSGM2023v75n3a061023

1991). The formation of this sedimentary-structural zone is the result of the collision between the African/Arabian plate with the Iranian plate, the process of which already started during the Mesozoic that was followed by the subduction of the Neo-Tethys and continued up to the continental collision during the Oligocene-Miocene (Berberian and King, 1981). Moreover, Reuter *et al.* (2009) expressed that these plates with widespread palaeobiogeographic and oceanographic consequences was the closure of the Tethyan Seaway which plays a significant role in establishing the connection between the Mediterranean sea and the Indo-pacific regions during the Oligocene-Miocene timespan (Figure 1c), wherein the marine Qom Formation was deposited at the north-eastern coast of the Tethyan Seaway (Reuter *et al.*, 2009). Nevertheless, the exact timing of the Neo-Tethys closure, known as the so-called terminal Tethyan event (TTE) (Schuster and Wielandt, 1999; Reuter *et al.*, 2009) is still debated whilst Adams *et al.* (1983) assigned it to the Aquitanian age, but it is attributed to the Burdigalin by several others authors (*e.g.* Rögl and Steininger, 1984; Rögl, 1999).

After petroleum discovery in the Serajeh and Alborz fields (Central Iran Basin) in 1934 (Rögl, 1999), The Qom Formation was studied from different aspects, especially with focus on the biostratigraphic, palaeogeographic and microfacies implications by many authors (*e.g.* Daneshian and Dana, 2007; Reuter *et al.*, 2009; Yazdi-Moghadam *et al.*, 2018a) in Central Iran.

The Qom Formation is chiefly composed of thick successions of limestones, marls, gypsum and siliciclastics from Rupelian-Burdigalian age in

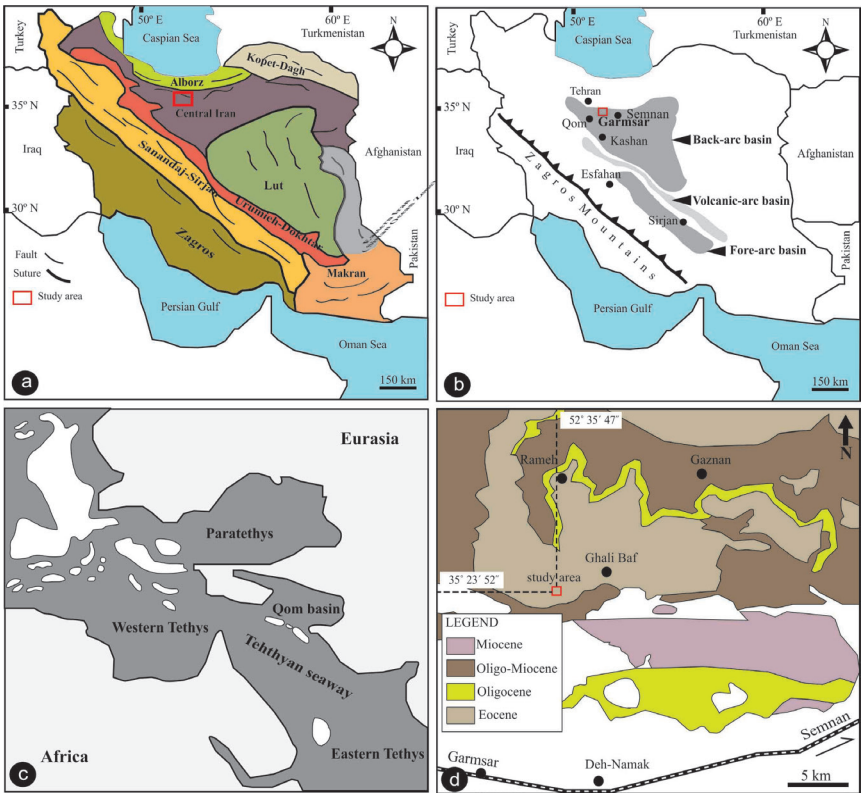

Figure 1 (a) General map of Iran showing the nine geologic provinces (adapted from Stöcklin, 1968); (b) A map showing the location of Esfahan-Sirjan fore-arc, Qom back-arc, and volcanic arc basins (modified from Schuster and Wielandt 1999; Reuter *et al.*, 2009); (c) Late Oligocene palaeogeography of the Tethyan Seaway and adjacent regions (modified from Harzhauser and Piller, 2007; Reuter *et al.*, 2009); and (d) Geographic map and location of the studied outcrop (Geological map of Semnan region, 1/250,000 from Nabavi, 1974).

the Central Iran (Reuter *et al.*, 2007). Furrer and Soder (1955) divided the type locality of the Qom Formation lithostratigraphic units near the Qom city into six members: basal limestone (a-member), sandy marl (b-member), alternating marl and limestones (c-member), evaporites (d-member), green marls (e-member), top limestone (f-member).

Thereafter, Soder (1959) divided the member "c" into four sub-members including, marlstones with intercalations of limestone (c-1), evaporates (c-2), shallow-water limestones (c-3) and green marlstones (c-4). However, Reuter *et al.* (2007) did not acknowledge these subdivisions of the c-member.

Finally, Stöcklin and Setudehnia (1991) based on the earlier work of Bozorgnia (1965), considered nine members (a, b, c-1, c-2, c-3, c-4, d, e, and f) for the Qom Formation and described lithological features of these members in the type area. However, Abaie *et al.* (1964) had expressed that the two members c-1 and c-3, were the main targets in petroleum discovery, wherein they increased the number of members to ten. In addition, Bozorgnia (1965) also suggested ten members based upon the lithological and palaeontological features of the Qom Formation.

In the type area, the Qom Formation was laid on the gypsiferous and evaporitic red beds (Lower Red Formation) conformably and overlaid conformably by the evaporitic red beds of Middle-Late Miocene age (Upper Red Formation) (Daneshian and Dana, 2007).

3. Material and methods

According to the interpretations proposed for the structural zones of Iran by Aghanabati (2006), the study area is situated in the north of central Iran zone. The Ghalibaf section (52°35'47"E; 35°23'52"N), is ~ 445m thick and situated ~5 km southwest of the Ghalibaf village, which is ~55 km northeast of Garmsar and ~85 km northwest of Semnan (Figure 1d). Based on the distinctive lithological features, the Ghalibaf section is differentiated into four lithological units: (1) the lower unit with a thickness of 120 m consists of medium to massive limestone and sandy limestone beds with lesser intercalations of marl, (2) this unit has a thickness of 105 m and is represented by marl and gypsum with intercalations of medium bedded limestone layers, (3) it is 140 m in thickness and predominantly composed of repetitive, medium-thick to massive bedded limestone and sandy limestone beds, and (4) the uppermost 80 m of the section consist of thick-massive marl and gypsum beds with intercalations of thin-medium bedded limestone. In total, 175 samples were studied and photographed under transmitted-light microscope (Olympus BX51). The petrographic thin-sections have dimensions 2.5 × 7.5 cm.

The available data were analysed to classify carbonate rocks following Embry and Klovan (1971) and Dunham (1962). Sequence stratigraphical analysis was performed according to the methods and principles of sequence stratigraphy proposed by some authors (Vail *et al.*, 1984; Galloway, 1989; Haq and Shutter, 2008). The larger benthic foraminifera were chiefly determined based on the taxonomic descriptions given after Loeblich and Tappan (1987), Hottinger (2007), and Sirel *et al.* (2013, 2020). The shallow benthic zones (SBZs) of the foraminiferal species follow Cahuzac and Poignant (1997). Finally, vertical and lateral patterns in biostratigraphy, primary physical structures, and sequence stratigraphy are used to interpret the changes in palaeoenvironmental settings.

4. Biostratigraphy

According to the biostratigraphy data, the Qom Formation carbonate platform is Early Miocene in age for the study section in the Garmsar area (Central Iran). These shallow-water limestones indicate the occurrence of Miocene larger foraminiferal assemblages belonging to the Aquitanian-Burdigalian (Figure 2) as described after Adams and Bourgeois (1967) within *Borelis melo* group-*Meandropsina iranica*

http://dx.doi.org/10.18268/BSGM2023v75n3a061023

assemblage zone and *Elphidium* sp. 14-*Miogypsina* assemblage subzone. These zones correspond to SBZ24-SBZ25. The most important larger foraminifera existing within these Qom Formation limestones are: *Praebullalveolina curdica*, *Borelis melo*, *Dendritina rangi*, *Meandropsina iranica*, *Elphidium* sp. 14, *Neorotalia viennoti*, *Miogypsina* sp., *Schlumbergina* sp., *Massilina* sp., *Archaias* sp., and *Pyrgo* sp. (Figure 3). Some species (*e.g.*, *Neorotalia viennoti*, *Schlumbergina* sp., and *Massilina* sp.) have a long stratigraphic range throughout the Oligo-Miocene. However, some porcellaneous and hyaline larger foraminifera (*Praebullalveolina curdica*, *Borelis melo*, *Meandropsina iranica*, *Miogypsina* sp., and *Elphidium* sp. 14) are index markers indicating the Late Aquitanian-Burdigalian age (*e.g.* Cahuzac and Poignant, 1997; Mohammadi, 2022). Daneshian and Dana (2007) reported the occurrence of both *Rotalia viennotti* and *Elphidium* sp. 14 in association with *Borelis melo curdica* within the younger strata

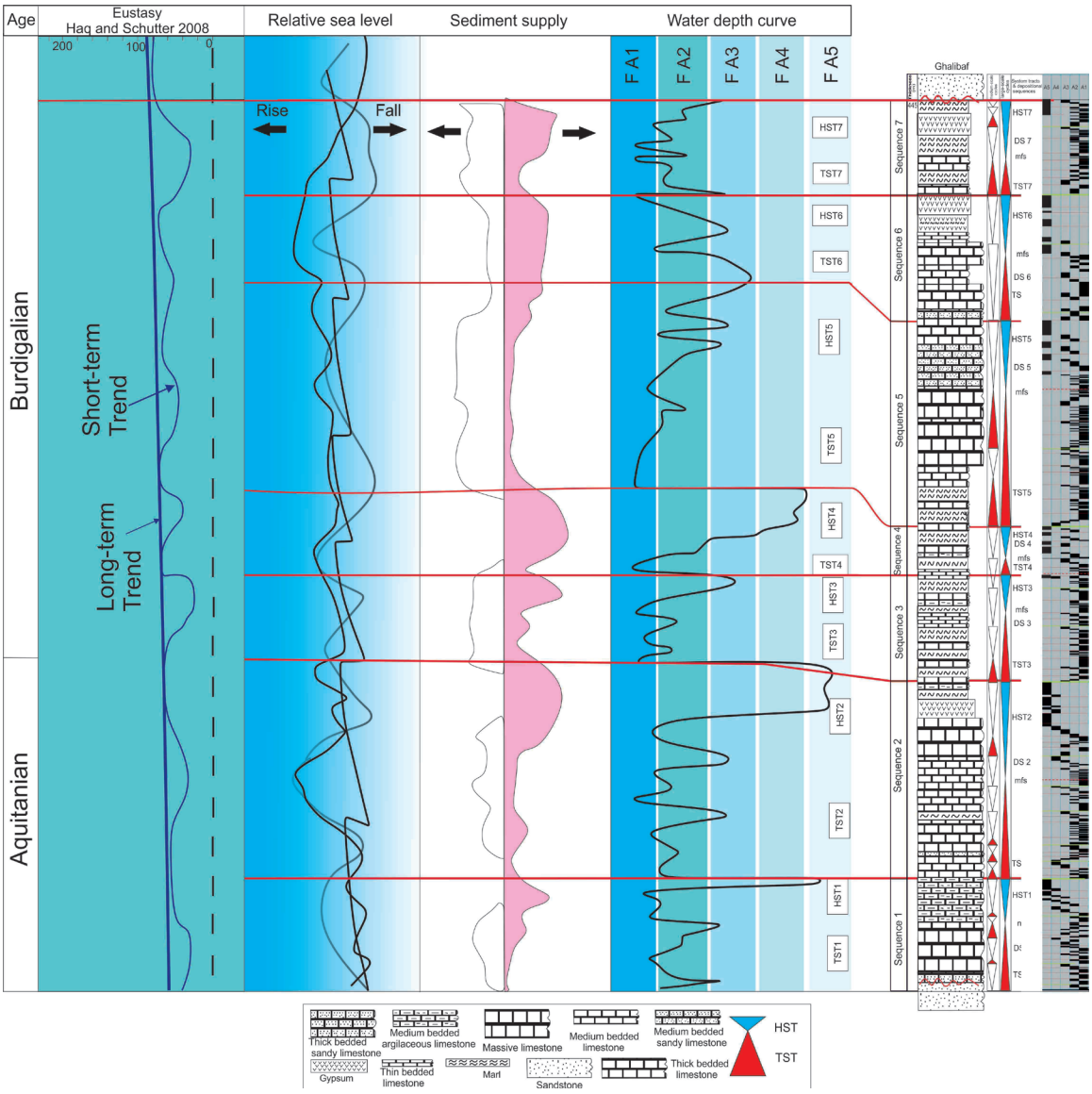

Figure 2 Sequence stratigraphy and depositional environment of the Qom Formation in the Ghalibaf section.

(probably Burdigalian) from the Qom Formation in Garmsar area. This coexistence is also observed in the present study. In the Ghalibaf section, the occurrence of *Praebullalveolina curdica* (Reichel, 1936-37) is reported for the first time from the shallow marine Miocene successions in Iran. This taxon has been previously described and figured under different names in the various localities of the Tethys areas, such as *Neoalveolina melo curdica* (Reichel, 1936-37, Turkey; Bozorgnia, 1965, Iran) and *Borelis curdica* (*e.g.*, Bignot and Guernet, 1976, Greece; Sirel, 2003, Turkey; Yazdi-Moghadam *et al.*, 2018a, 2018b, Iran). *Borelis curdica* (Reichel) had been transferred to *Praebullalveolina* (Sirel and Acar, 1982) as *Praebullalveolina curdica* (Reichel, 1936,-37) (see Sirel *et al.*, 2020, for further details). Overall, the study section is included in the SBZ24-SBZ25 equivalent to the Late Aquitanian-Burdigalian timespan.

5. Microfacies analysis

5.1 DESCRIPTION

In the Ghalibaf succession, a comprehensive assessment of field and petrographical observations along with a detailed thin-section analysis has allowed for the recognition of five facies associations (FAs 1-5) and twenty-one microfacies types. Based on the palaeoenvironmental and sedimentological analysis, five FAs from the land to the sea are lagoon, platform-margin sand shoals, margin facies, upper slope facies, and lower slope facies:

5.1.1 DEEP MARINE TO LOWER SLOPE FACIES ASSOCIATION (FA1)

This FA shows a vertical, heterolithic alternation (5-10 m), comprising argillaceous mudstone, thin to medium organic-rich calcareous shale, marl to marly limestone, packstone interbedded limestone and shale, and wackestone. The lower boundary is mainly erosive, although there are graded bedding structures in the limestone beds (Figure 4a-d). The predominant FA1 are pelagic characterized by calciturbidites and breccia. The thickness of the sedimentary layers and the size of skeletal and non-skeletal fragments decrease toward the basin.

Bioclasts and detrital grains are represented by small fragmented bioclasts with crinoids, sponge spicules, planktonic foraminifera, brachiopods, framboidal pyrite crystals, and silt-sized quartz. Based on the frequency, the matrix between carbonate grains, and the type of carbonate grains, FA1 is divided into three microfacies:

5.1.1.1 Planktonic foraminifera wackestone (A1)

This microfacies is observed within thin to medium bedded dark limestones. They are composed of lime mud and planktonic foraminifera (Figure 4a). The chambers of planktonic foraminifera are filled with pyrite, sparry calcite, and lime mud. In addition, the subordinate components are small benthic foraminifera, bivalves shells, and echinoid spines. It is devoid of any shallow water fauna. The lime mud matrix of this microfacies is sometimes very dark due to the presence of organic matter. This microfacies also contain glauconite, which is characterized by a frequency of more than 5% of grains, angularity, and a pale green to yellowish color (Figure 4a).

5.1.1.2 Graded bedding and Bouma sequence packstone with planktonic foraminifera (A2)

This microfacies consists of light to dark grey limestones. It is mainly represented by planktonic foraminifera with a frequency of 50 to 60%. The subordinate components are small benthic foraminifera, broken shells of bivalves, and sponge spicules (Figure 4b-h). This microfacies is well-defined by both of shallow (small miliolids) and deep (planktonic foraminifera) water faunal contributors (Figure 4e) and other components such as glauconite and opaque minerals comprising less than 1% of grains. In this microfacies, the fining upward cycle (Unit A of Bouma sequence

http://dx.doi.org/10.18268/BSGM2023v75n3a061023

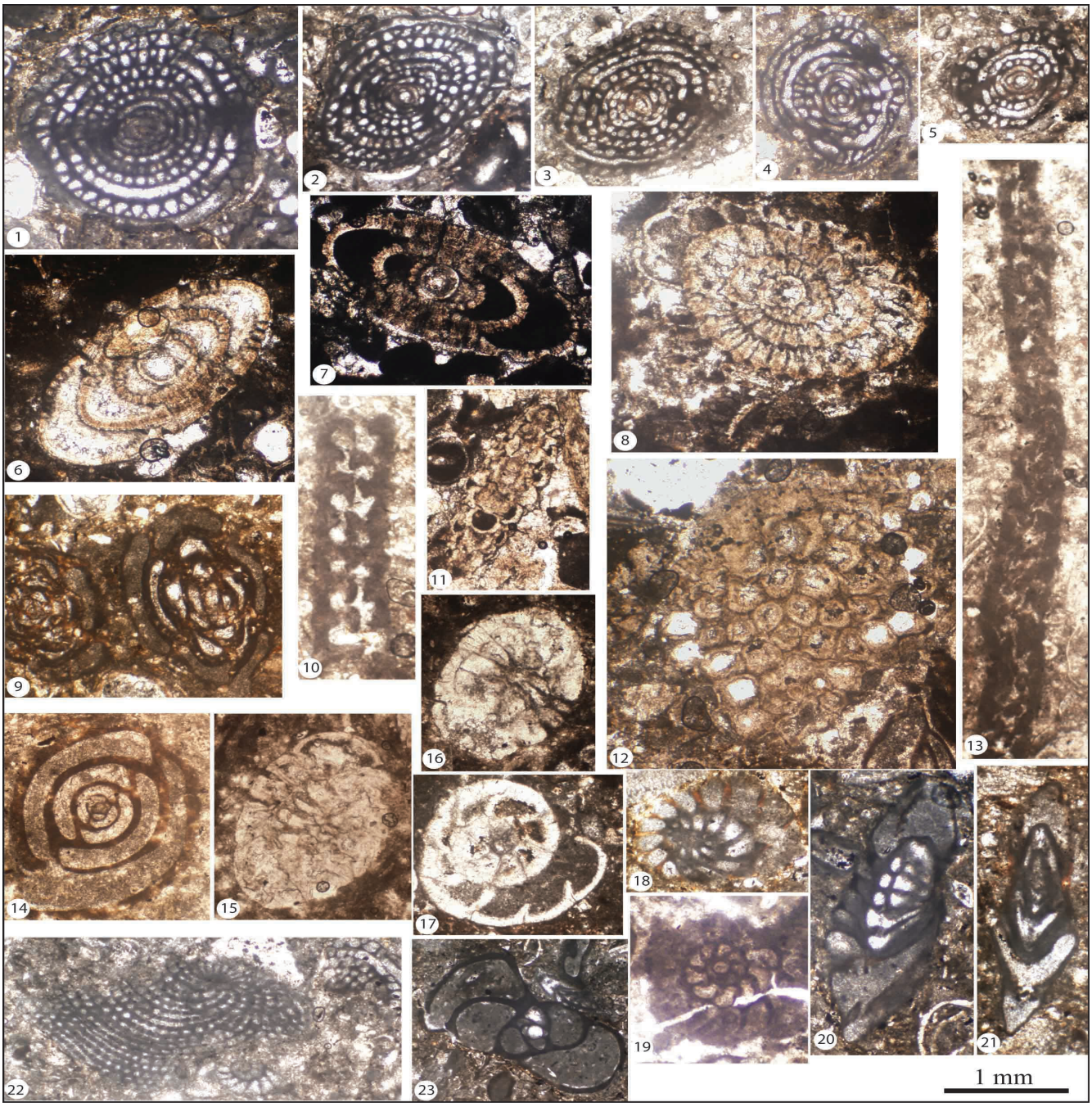

Figure 3 (1-3) *Praebullalveolina curdica* (centered and non-centered axial sections, Burdigalian); (4-5) *Borelis melo* (Axial section, Burdigalian); (6-8) *Elphidium* sp. 14 (Axial and subequatorial section, slightly oblique, late Aquitanian-Burdigalian); (9) *Schlumbergerina* sp. (sub-longitudinal section, late Aquitanian-Burdigalian); (10, 13) *Meandropsina iranica* (Henson; uncentered incomplete axial section, Burdigalian); (11-12) *Miogypsina* sp. (slightly oblique equatorial and incomplete sub-axial section, late Aquitanian-Burdigalian); (14) *Pyrgo* sp. (proximally axial section, late Aquitanian-Burdigalian); (15-17) *Neorotalia viennoti* (Greig) (slightly oblique axial and equatorial sections, late Aquitanian-Burdigalian); (18-21) *Dendritina rangi* (d'Orbigny) (sub-axial and equatorial, slightly oblique sections, Burdigalian); (22) *Archaias* sp. (uncentered incomplete equatorial section, late Aquitanian); and (23) *Massilina* sp. (proximally axial section, Burdigalian).

http://dx.doi.org/10.18268/BSGM2023v75n3a061023

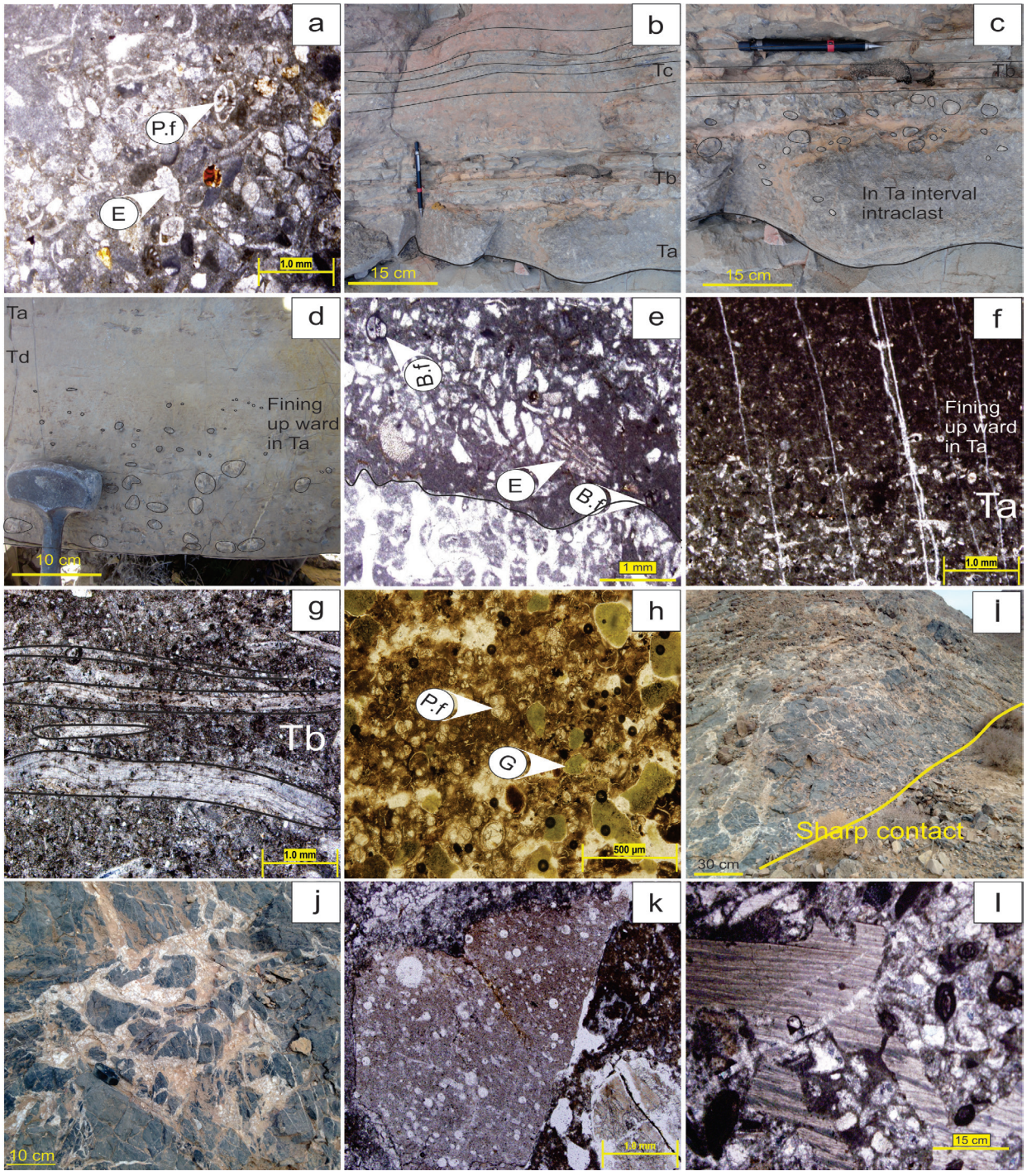

Figure 4 Field and photomicrographs of FA1: a) Planktonic Foraminifera wackestone microfacies (A1): photomicrograph showing mudstone texture with thin-shelled bivalves, crinoids; b-d) Field photograph of graded bedding and Bouma sequence packstone with planktonic foraminifera with showing erosional base (b, c), graded bedding (d), incomplete Bouma sequence (Bouma, 1962); e-h) Photomicrograph of microfacies A2; i and j) Field photograph of breccia (A3); k and l) Photomicrograph showing grey breccia with angular clasts. E: Echinoid, P.f: Pelagic Foraminifera, B.f: Benthic Foraminifera, G: Glauconite, Ta: Unit a of Bouma sequence, Tb: Unit b of Bouma sequence.

http://dx.doi.org/10.18268/BSGM2023v75n3a061023

in Figure 4b-h) and the undamaged and broken bioclastic components can be observed. These components are parallel to each other, indicating displacement after deposition (Unit B of Bouma sequence). Additionally, field evidence shows the presence of a ripple lamination (Unit C of the Bouma sequence in Figure 4b-h).

5.1.1.3 Breccia (A3)

These breccia beds are composed of angular polymictic fragments. The fragments of breccia beds have a different lithological composition from the host rock. The clasts are characterized by mudstone and bioclastic packstone-grainstone textures with grain sizes varying from a few millimeters to centimeters. The breccia beds are mostly clast-supported (Figure 4i-l). The unique feature of these rocks are chaotic internal fabrics. Breccia consists of unsorted intraformational fragments. In general, these breccia beds have sharp erosional bases and lenticular geometry. These breccias are intercalated with calciturbidites that contain lens-shaped bodies or channels.

5.1.2 UPPER SLOPE FACIES ASSOCIATION (FA2)

This FA is characterized by medium to thick beds with alternating thickness of 6 to 10 m, grey to dark grey graded (intra-skeletal) floatstone and rudstone, and graded bioturbated Bouma sequence. Sedimentary structures in the FA2 include graded bedding, flute marks and erosional base. The frequency ratio of coarse carbonate layers and the general pattern of thickness decrease towards the deeper parts of the basin. The identified microfacies in the FA2 are as follows:

5.1.2.1 Intraclast bioclastic rudstone-floatstone (B1)

This microfacies comprises dark grey medium-bedded limestones (floatstone-rudstone alternation). It is graded and contains a high diversity of organisms, including brachiopods, crinoids, bivalves, echinoids, benthic foraminifera, calcareous red algae and corals (Figure 5a-b). Predominantly, rudstone-floatstone layers are represented by intraclasts and allochems containing poorly-sorted fragments with sub-rounded to unequal outlines (2-3 mm in size; Figure 5b-c). Sedimentary structures include graded bedding and erosional base (Figure 5a). These fragments are commonly scattered in the sparry calcite and micritic matrix.

5.1.2.2 Bioclastic floatstone (B2)

This microfacies is formed of dark grey limestones with thin to medium bedded texture (floatstone). It is characterized by the abundance of skeletal fragments of corals, brachiopods, calcareous red algae, bivalves, and echinoids and a small amount of intraclasts and peloids in a micritic matrix (Figure 5d-e). The bioclasts are densely packed, moderately sorted, fragmented and abraded. The degree of articulation is high. The well-rounded convex-up valves are preserved aligned with the bedding and oriented in the pavements.

5.1.3 MARGIN FACIES ASSOCIATION (FA3)

This FA displays coarsening-upward succession with a thickness 6-10 m. It also contains grey limestone beds with medium to thick bedding, which are mainly composed of corals and bivalves. This FA3 is identified by parallel and planar laminations, and HCS (Figures 5f, g, j, k). The FA3 consists of two microfacies (C1 to C2) separated according to the type and frequency of the allochems.

5.1.3.1 Coral boundstone with red algae (C1)

This microfacies is characterized by massive and thick-bedded dome-shaped massive, dark grey limestones. Corals with a regular skeletal framework are the main components of this microfacies. Skeletal fragments, such as calcareous red algae, brachiopods, and echinoids, are the subordinate components (Figure 5h-i). Summarizing, it can be said that the coral assemblages of this microfacies play an important role in forming the barrier reefs (Figure 5h).

http://dx.doi.org/10.18268/BSGM2023v75n3a061023

5.1.3.2 CORAL FRAMESTONE (C2)

This microfacies consists of massive and thick-bedded dome-shaped massive, dark grey to cream coloured limestones. The major component of this microfacies is corals with calcite cement. Other subordinate components are bivalves and benthic foraminifera. A small amount of quartz in fine sand size grains is also present (Figure 5l). These corals have formed a continuous framework and can be observed over long distances (Figure 5j-k).

5.1.4 PLATFORM-MARGIN SAND SHOALS FACIES ASSOCIATION (FA4)

This FA mainly comprises coarsening-upward successions (6-10 m). It contains grey limestone (bioturbated) beds with medium to thick-bedded texture. Planar lamination, and HCS are the dominant features of this microfacies assemblage (Figure 6a-c). Skeletal assemblage of this limestone is composed of packstone, floatstone, and locally grainstone, including bioclasts such as peloids, corals, brachiopods, sponges, echinoids, bryozoans and non-skeletal ooids. The FA4 consists of seven microfacies.

5.1.4.1 Bioclastic floatstone rudstone (D1)

This microfacies is characterized by rudstones to grey medium-bedded floatstones with planar lamination and micro-HCS. The main components of this microfacies are bivalves shells (4 to 20 mm in diameter) with a random orientation. Bioclasts are broken and somewhat sorted. They mainly contain benthic foraminifera, brachiopods, bryozoans and echinoids, sometimes sizes up to 2 mm (Figure 6d). Pellets are also present as subordinate components.

5.1.4.2 Intraclastic bioclastic grainstone- rudstone (D2)

This microfacies is identified by grey to dark grey limestone with a thick-bedded and relatively well-sorted grains. Typically, this microfacies represents a coarsening-upward character with rare cross laminations and massive bedding. The main skeletal and non-skeletal components are chiefly made up of bioclastic (including echinoids, brachiopods, red algae, and bivalves) and intraclastic fragments. The grains are well-sorted, and the micrite is removed and filled with sparry calcite cement (Figure 6e-f).

5.1.4.3 Crinoid grainstone (D3)

This microfacies is identified by grey limestone with thick-bedded texture and contains relatively well-sorted grains. The main components are highly abundant crinoids and echinoid tests (Figure 6g -h). The subordinate components commonly contain brachiopods and bivalve fragments.

5.1.4.4 Intraclastic grainstone (D4)

This microfacies features thin-bedded, dark grey limestones. It contains orthochem-rich, moderately to well-sorted, coarse- to medium-grained limestones. Intraclasts as sub-rounded and sorted grains are the main non-skeletal components of this microfacies (Figure 6i). Skeletal fragments are small and mainly composed of bivalves and echinoids.

5.1.4.5 Bioclastic ooidal grainstone (D5)

This microfacies comprises cream-colored, massive, and thick-bedded limestones and has parallel bedding (Figure 6j-k). Ooids are more abundant than other allochems with cements that fills the interparticle porosities. The skeletal allochems consist of miliolids and bivalves. The composite ooids are also present in this microfacies, in which the nuclei of most ooids are made of brachiopod and echinoid tests (Figure 6k).

5.1.4.6 Peloidal bioclastic grainstone (D6)

This microfacies is characterized by cream-colored, massive, and thick-bedded limestones. Bioclasts are more abundant than peloids, and their frequency reaches more than 50%.

http://dx.doi.org/10.18268/BSGM2023v75n3a061023

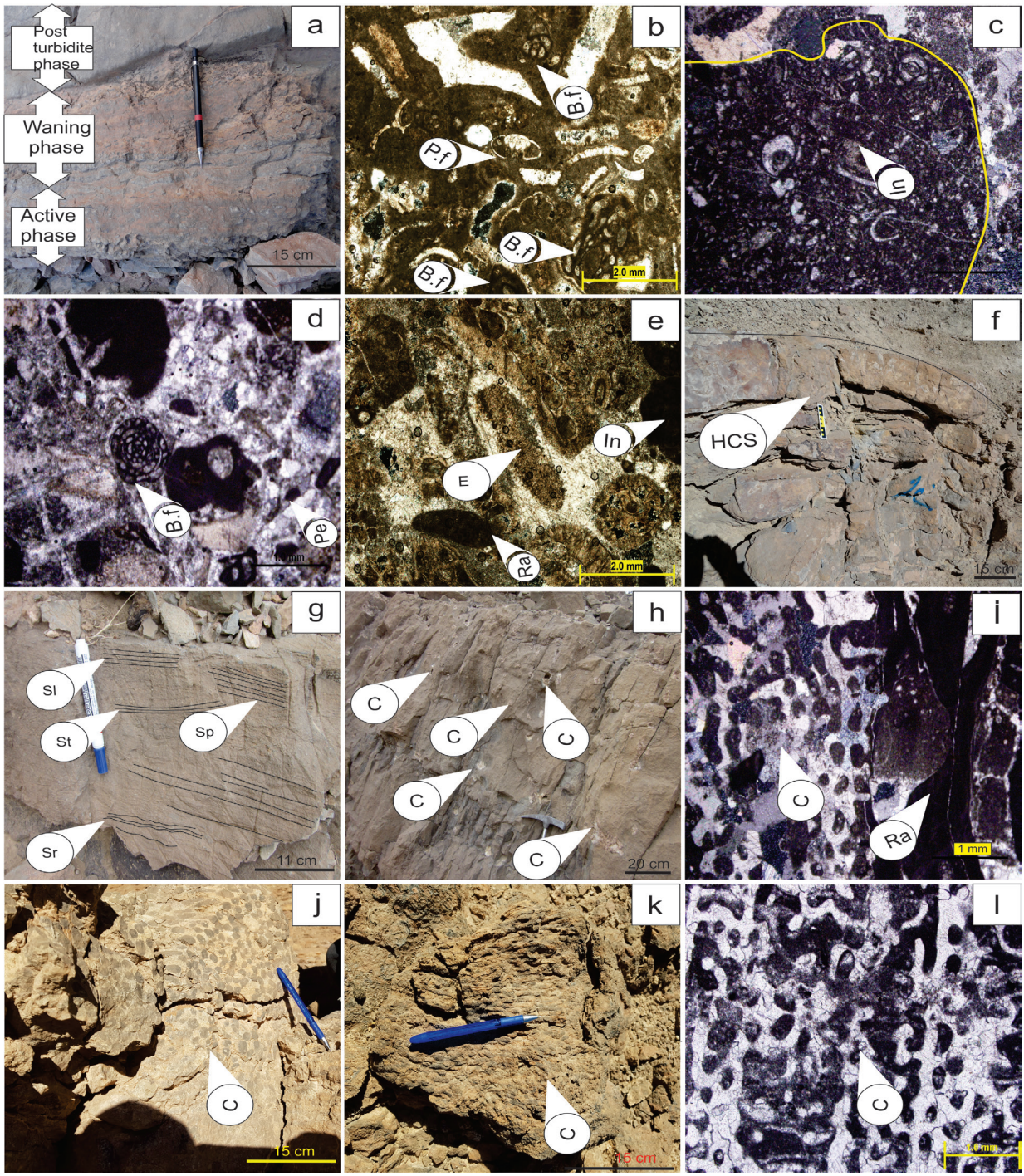

Figure 5 Field and photomicrographs of FA2 (a-e) and FA3 (f-l): a) Field photograph of intraclast bioclastic rudstone-floatstone microfacies (B1) in Bouma sequence; b and c) Photomicrographs of microfacies B1, allochems consist of benthic and pelagic foraminifera and intraclast; d and e) Photomicrographs of bioclastic floatstone microfacies (B1), the abundance of skeletal fragments of, red algae, bivalves, and echinoids; f and g) Field photograph of FA3 with planar lamination, wave Rippled and HCS; h and i) Field and photomicrographs of coral boundstone with red algae (microfacies C1). Corals show a biostrome growth pattern. The space between the grains is filled by calcite cement; and j, k) Field photograph of Coral framestone (C2); L) Photomicrograph of Coral framestone. Corals are as patch reef. P.f: Pelagic Foraminifera, B.f: Benthic Foraminifera, C: Coral, HCS: Hummocky Cross Stratification; Sp: Planar stratification; St: Trough stratification Sr: Ripple stratification; Sl: Laminar stratification; In: Intraclast; Pe: Peloid; Ra: Red algae.

http://dx.doi.org/10.18268/BSGM2023v75n3a061023

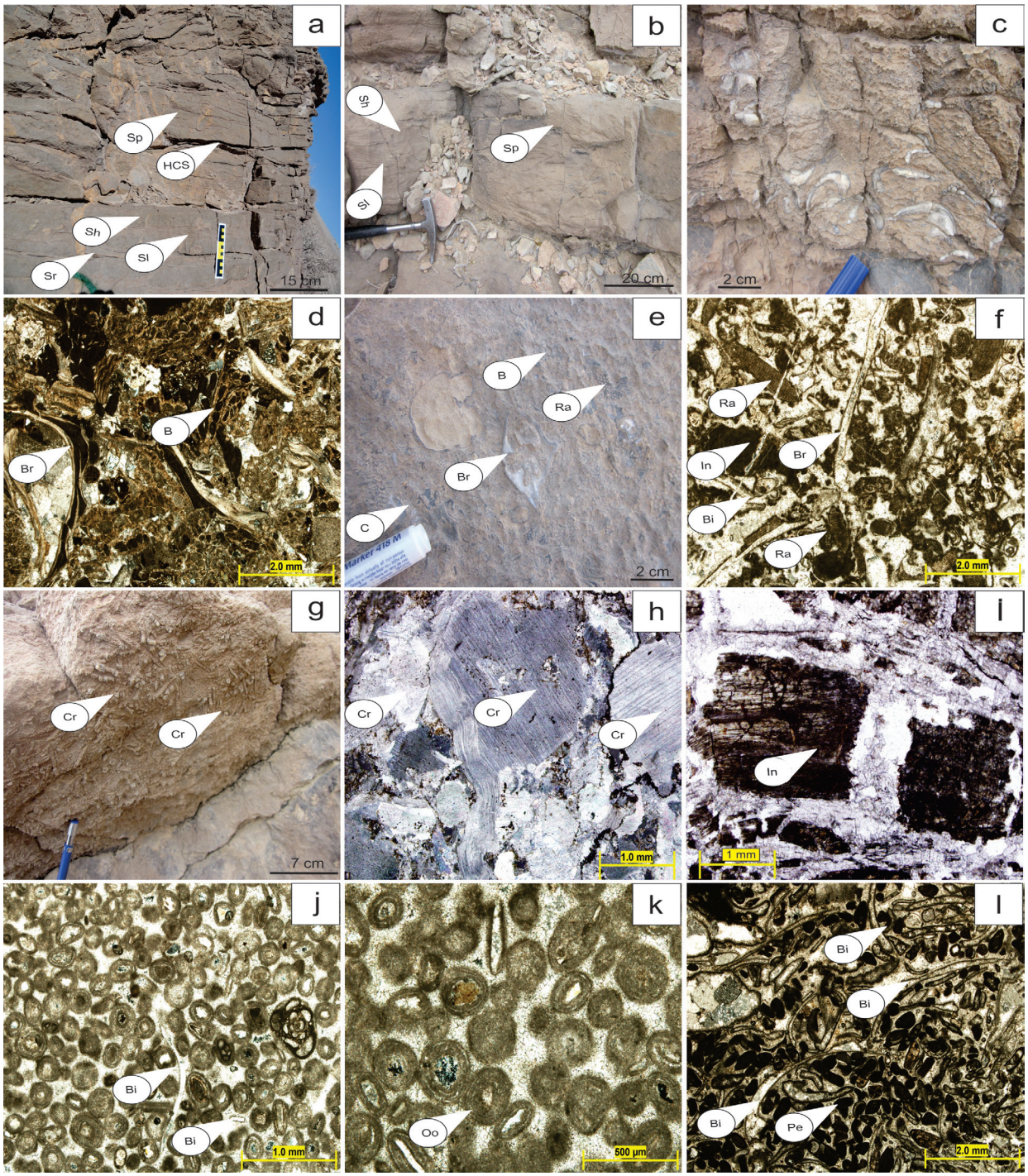

Figure 6 Field and photomicrographs of FA4: a-c) photomicrographs of bioclastic floatstone-rudstone with shell fragments (c), planar lamination, horizontal and lamination stratification, wave rippled and micro HCS (a, b); d) Photomicrograph of microfacies D1; e and f) Field and photomicrographs of intraclastic bioclastic grainstone-rudstone, the space between the grains is filled by calcite cement; g and h) Field and photomicrographs of crinoid grainstone, the major component is crinoid. The space between the grains is filled by calcite cement; i) Photomicrograph of intraclastic grainstone; j, k) Photomicrographs of bioclastic ooidal grainstone, allochems consist of ooids and bivalves with space between them is filled with calcite cement; and l) Photomicrograph of peloidal bioclastic grainstone. Br: Brachipod, Ra: Red algae, E: Echinoid; In: Intraclast; Pe: Peloid; Oo: Ooid; C: Coral, B: Bryozoan, Bi: Bioclast; Pe: Peloid; HCS: Hummocky Cross Stratification; Sp: Planar stratification; Sh: Horizontal stratification; Sr: Ripple stratification; Sl: Laminar stratification.

http://dx.doi.org/10.18268/BSGM2023v75n3a061023

Bioclasts consist of bivalves and echinoids. Calcite cementation is abundant in this microfacies (Figure 6l). In addition, the peloids are elongated to spherical with a diameter size between 0.05 mm and 0.1 mm.

5.1.5. LAGOON FACIES ASSOCIATION (FA5)

This FA contains thin to thick-bedded wackestone/mudstone to packstone. The FA5 comprises various skeletal fragments such as imperforate benthic foraminifera, gastropods, bivalves, echinoids, brachiopods and bryozoans. It also contains low amount of non-skeletal fragments, including pellets, ooids, and intraclasts that are scattered in a micritic matrix. Detrital quartz is occasionally detected in this FA based on the abundance and type of matrix and allochems. The FA5 is divided into microfacies E1 to E3, describedas follows:

5.1.5.1 Sandy bioclastic mudstone (E1)

This microfacies comprises thin-bedded grey mudstone. Bioclasts are distributed in a muddy matrix. They are mainly composed of lime mud containing imperforate benthic foraminifera (miliolids) and bivalves along with more than 10% quartz (Figure 7a-b).

5.1.5.2 Interaclast bioclastic wackestone/packstone (E2)

This microfacies is identified by thin-to medium-bedded cream-colored limestones. Besides, they contain intraclast-rich layers with a thickness of 0.5 mm to 2 mm. Bioclasts are composed of bivalves, miliolids, benthic foraminifera and green algae. Intraclasts are displayed in moderately sorted beds mainly stacked through lenticular and laterally discontinuous units with erosional bases. Moreover, the skeletal components with low abundance are observed floating in lime mud (Figure 7c-d).

5.1.5.3 Bioclastic miliolid packstone (E3)

This microfacies is characterized by thick to massive bedded cream-colored limestones. The main biogenic components are miliolid foraminifera, bivalves and calcareous red algae (Figure 7e-f). Other bioclastic fragments (brachiopods and bryozoans) are mainly well-preserved.

6. Depositional system

6.1 INTERPRETATION OF LOWER SLOPE FA

The occurrence of planktonic foraminifera and the absence of benthic organisms indicate an open marine environment. In addition, good preservation of the planktonic forams can be indicative of an open marine environment with low energy (see Warren, 2000; Flügel, 2010; Bover-Arnal *et al.*, 2015). The presence of pyrite and a dark matrix of organic matter with the abundance of mud in the FA1indicate low energy conditions and a low oxygen environment. These factors suggest a deep palaeoenvironment for the deposition of the limestone and sedimentation under reducing conditions (Tucker and Wright, 1990; Flügel, 2010; Bayet-Goll *et al.*, 2022).

In the FA1, a low sedimentation rate, reducing conditions, and normal salinity are the prerequisite conditions associated with the formation of glauconite, which can be formed in a deep environment (Flügel, 2010). These types of breccia are usually created in deep sea areas below the slope and in the basin under the influence of deep-water muddy gravity flows and sediment-laden gravity currents (Haas *et al.*, 2010; Bayet-Goll *et al.*, 2023).

Re-deposited carbonates are generated when the sea level rises (Tucker, 1985). At this time, the carbonate production rate is high, and the grains are compacted together but not cemented (Bayet-Goll *et al.*, 2023). If the thickness of the sediments increases excessively and the front slope of the platform is steep due to reduced stability, these deposits will move downwards (Bayet-Goll *et al.*, 2023). Alternating deep marine and shallow deposits indicate the displacement and redeposition of shallow deposits in the deep parts (Figure 4e). The presence of graded bedding, the parallel arrangement of bioclastic fragments, and the

http://dx.doi.org/10.18268/BSGM2023v75n3a061023

ripple lamination in this microfacies (A2) indicate the Bouma sequence's Ta, Tb, and Tc divisions (Figure 4b-d) (Eberli, 1987). Compared with the rimmed carbonate platform model (Kenter *et al.*, 2001, 2005), the FA is deposited at the lower slope part below the storm wave base.

6.2 INTERPRETATION OF UPPER SLOPE FA

A mixture of resedimented shallow-marine debris with dominant deep marine fauna, erosive base, normal grading, and incomplete Bouma intervals are recorded in the upper slope in this FA. These evidences indicate discontinuous transportation from a carbonate platform mainly by turbidity currents and deposition into the proximal to distal zones of the outer ramp, which passes to a gentle slope zone (Mutti *et al.*, 2003). Thus, this facies association is deposited on the carbonate platform slope. In accordance with the rimmed carbonate platform model (after Kenter *et al.*, 2005; Flügel, 2010), this facies association is deposited below the fair-weather wave base (FWWB) and in the upper slope.

The sedimentary profile, together with the presence of stacking patterns, shelf-edge trajectories and the arrangement of sedimentary layers at the edge of the shelf suggest sedimentation on the carbonate platform slope. The high abundance of intraclasts and coral fragments along with the erosive bases show the effect of episodic erosion in this part of the sequence. These evidences can be the influence of high energy currents that could be the most important factor in the coarse size of grains from the upper slope and the absence of a high mud matrix in this FA.

In addition, the poor degree of sorting and the high fragmentation of these deposits suggests the proximity to the source of sediment production, including the margin and sand bars (Della Porta *et al.*, 2002, 2003). Moreover, the presence of intraclasts along with the skeletal fragments with high fragmentation and abrasion can express the reworking of sediments by waves from a nearby origin (Kenter *et al.*, 2005).

6.3 INTERPRETATION OF MARGIN FA

This FA is deposited in the upper part of the carbonate platform, which separates the open marine environment from the lagoon and corresponds to the rimmed-carbonate platform margins. According to the rimmed carbonate platform model, this FA is constituted on the platform margin reefs, close to the fair-weather wave basin in the euphotic zone. The microfacies C2 is formed by in-situ organisms (colonial corals) and suggests a reef environment. The reef microfacies that form on the platform margin belong to the barrier reefs between the middle and inner shelf (see Wilson, 1975). These reefs are placed above the normal FWWB (Geel, 2000).

The presence of well-preserved coral communities, in-situ growth patterns, and high skeletal diversity indicates a warm shallow-marine environment with optimal hydrodynamic energy conditions close to the FWWB (Fürsich and Pandey, 2003; Kenter *et al.*, 2005; Flügel, 2010). Additionally, the occurence of bioclastic beds of the barrier with bioherms (C1 and C2) indicates the presence of temporary high-energy conditions or seasonal storms at the platform edge (Fagerstrom, 1991). In this FA of the Miocene deposits, reefs are known as barrier reefs in both bioherm and biostrome morphological patterns (Fagerstrom, 1991). Hence, the expansion of bioherm from the Miocene study interval can be indicative of steep margins in the lower and upper slope.

6.4 INTERPRETATION OF PLATFORM-MARGIN SAND SHOALS FA

An important feature of D1 to D7 microfacies is the absence of a calcareous matrix and the presence of coarse grains, indicating high energy during deposition (Fürsich and Pandey, 2003; Van Buchem *et al.*, 2010; Bover-Arna *et al.*, 2015). The biodiversity in these microfacies suggests an initial sedimentary environment with good water circulation, normal salinity, and sufficient oxygen (brachiopods, sponges, echinoids, bryozoans) (Kenter *et al.*, 2001, 2005).

http://dx.doi.org/10.18268/BSGM2023v75n3a061023

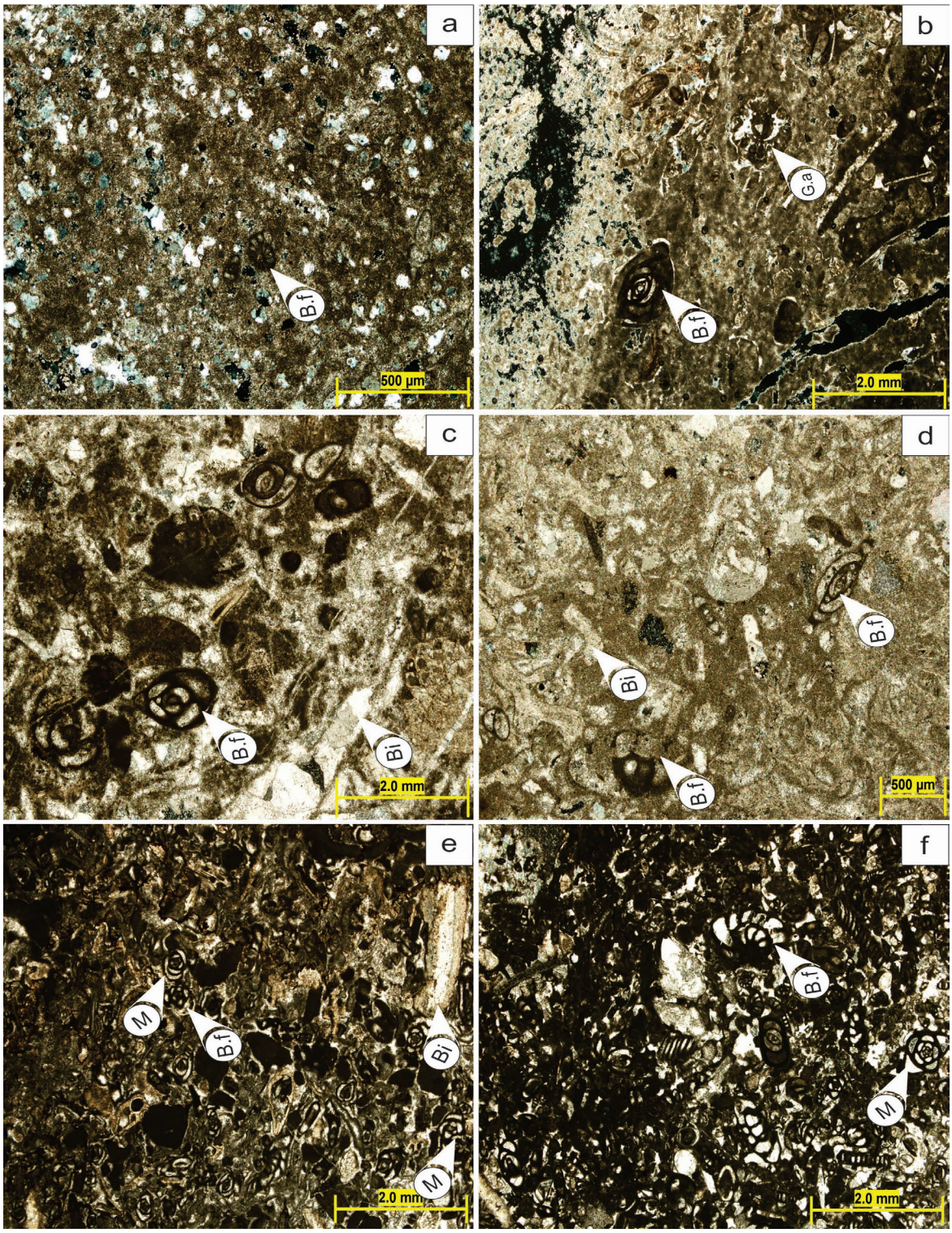

Figure 7 Photomicrographs of FA5: a and b) Photomicrographs of sandy bioclastic mudstone, bioclasts containing imperforate benthic foraminifera, green algae and bivalves; c and d) Photomicrographs of interaclast bioclastic wackestone/packstone, bioclasts consist of bivalves, miliolids, benthic foraminifera; e and f) Photomicrographs of bioclastic miliolid packstone, the major component is miliolid and other bioclasts consist of bivalve, benthic foraminifera and red algae. Bi: Bioclast; B.f: Benthic Foraminifera, G.a: Green algae; M: Miliolid.

http://dx.doi.org/10.18268/BSGM2023v75n3a061023

Additionally, the fossil contents (corals, brachiopods, sponges, echinoids, bryozoans) and sedimentary structures such as planar lamination and HCS indicate markers for the high-energy levels of the sand shoals from the platform margin. Moreover, the presence of grainstone-rudstone indicates the high energy environments such as ridges. In some microfacies, the presence of large amounts of aggregates, intraclasts, and grainstone-rudstone suggests sedimentation under shallow and high-energy conditions such as ridges and barriers (Laursen *et al.*, 2009). The grains in this FA are well sorted and rounded, indicating continuous water flow activity.

Additionally, large amounts of ooids show deposition in shallow water under highly energetic conditions such as ridges and bars (Geel, 2000; Bachmann and Hirsch, 2006; Li *et al.*, 2018; Kikichi *et al.*, 2018). The high abundance along with sorted and rounded skeletal fragments, suggests that this FA formed above the FWWB influences the constant wave activity. These conditions occur especially in winnowed platform edge sands and sand bars of the inner ramp (Flügel, 2010).

According to the rimmed carbonate platforms model, this FA was deposited in the platform margin sand shoal and bars in the photic zone and above the FWWB.

6.5 INTERPRETATION OF LAGOON FA

This FA shows large amounts of miliolids, porcelanous imperforate benthic foraminifera, peloids, and green algae together with lime mud between the particles (see Fournier *et al.*, 2004; Brandano, *et al.*, 2010). These evidences suggest deposition in a lagoon and the inner shelf with low-depth, relatively limited circulation of water, relatively high salinity and low energy that is in accordance with the standard microfacies described by Wilson (1975). This FA also contains non-skeletal fragments such as peloids that represent a lagoon environment. The mud intraclasts are found and show evidence of basin organisms, such as sponge spicules and radiolarians, suggesting their large displacement in front of the barrier.

In addition, some fossils belonging to areas with limited water circulation such as miliolids and open marine organisms (e.g., brachiopods, bryozoans, and echinoids) are also present, with their frequency reaching 10-15%. The presence of these fossils in lagoon environments is probably due to transport by storm activities (Tucker, 1985). Lagoonal fossils and marine bioclasts, beside intraclasts show deposition at the end of the platform margin within a lagoon environment.

6.6 DISCUSSION

6.6.1 SEDIMENTARY MODEL

The Qom Formation basin developed on the eastern continental margin of Tethys during the Oligo-Miocene and is a remarkable Paleogene carbonate platform, in which alternating siliciclastics and carbonates have been deposited. Five important facies associations (FAs) are recognized. These FAs are classified into 21 microfacies and show a great amount of larger foraminifera (Figure 8). Microfacies changes demonstrate a depth gradient from shallower to deeper basins through the distribution of foraminifera and other primary components.

Gradual changes in microfacies are accompanied by water deepening from the inner- to the middle-shelf basins. Additionally, the presence of slope FA and well-developed margins indicates the presence of a low-gradient shelf. This perspective represents the inner and middle shelf settings (above FWWB). The faults area, in terms of tectonic history in the Ghalibaf section, has caused apparent discontinuities in the microfacies of the exposed rock units. Along the west, this fault zone is composed of the Paleocene sequence, although just the Upper Red Formation (URF) has formed in the study area (Berberian and King, 1981; Alavi, 1994). This orogeny has resulted in a major alteration in the structure and significant removal of the rock units in the study region. These basins

http://dx.doi.org/10.18268/BSGM2023v75n3a061023

have received erosion-based sediments generated by the formerly uplifted regions. This tectonic activity has deepened the sedimentary basin and increased the transition from continental to marine microfacies in the Oligocene-Miocene.

However, since the sedimentary basin has been unrested, the term multiphasic sedimentary basin should be used for the Oligo-Miocene timespan. This facies model indicates a slight slope from the inner shelf to the middle shelf due to the distribution patterns of foraminifera and other skeletal components. It can also be attributed to the lack of slumpy sediments and reef microfacies.

The existence of marginal reef development, the presence of high-energy grainstone microfacies, resedimentation (calciturbidites) and the sharp separation of slope from the shoreline into deeper water are consistent with the conditions in which the Qom Formation has been deposited on a carbonate shelf. FAs denote lagoon, platform-margin sand shoal, margin, upper slope, and deep marine to lower slope environments.

The textural features and dominance of miliolids, bivalves, green algae along with the existence of some micritized fragments indicate a very shallow-marine back shoal basin. These factors suggest a semi-restricted lagoon adjacent to a shoal with almost low currents (Taghdisi Nikbakht *et al.*, 2019). This high-energy inner-shelf (platform-margin sand shoal FA) is characterized by the appearance of non-skeletal carbonate grains (peloids, ooids, and intraclasts), skeletal grains (echinoids), bryozoans and red algae in a packstone to grainstone texture (Nasiri *et al.*, 2020).

The upper slope and deep marine to lower slope also are indicated by fragmented and fine-grained bioclasts such as spiculites. Moreover, bioclastic wackestone shows a sedimentation zone consistent with a transition from deep marine to lower slope belts.

Microfacies analysis revealed that the deeper zones of the shelf (deep marine to lower slope) have a high amount of laminated fine-grained wackestones, normal-graded wackestone/packstone beds as distal-turbiditic deposits, resedimented fine- to medium-grained packstones with small benthic foraminifera.

This sharp slope shows a zone with high deposition rates due to the increase in the volume of finer-grained deposits delivered to the marine basin through the reworking and offshore transport of sediments from the shallower mesophotic zone. In general, the lower shelf slope is dominated by muddy calciturbidites, fine-grained pelagic wackestone/mudstone, and intra-formational breccia. These observations provide evidence of resedimentation through the bottom currents and an increased supply of platform-derived deposits by gravity currents.

Besides, some intense reworking and re-deposition of platform-derived materials have been recorded in the slope settings (Pedley, 1998). The abundance of carbonate and argillaceous mud and the poorly sorted grains in this deep marine FA is indicative of a quiet water and low-energy environment (Nasiri *et al.*, 2020). Consequently, the carbonate successions of the Qom Formation represent a shelf with well distinguished inner, mid and outer shelves (Figure 8).

6.6.2 SEQUENCE STRATIGRAPHY

Detailed stratigraphic and sedimentological studies of the Qom Formation sediments in the northwest of Semnan led to the recognition of seven third-order depositional sequences identified by sequence boundaries (Figures 2 and 9). The thickness of each system tract ranges from tens to several tens of meters, depending on the palaeogeographic position and subsidence within the basin. Sediments have mostly been deposited during the highstand. The highstand systems tract (HST) is divided into a progradation (normal regression) late highstand systems tract (LHST) and an early highstand systems tract (EHST). The EHST fills the vertical accommodation space. In the study area, the transgressive systems tract (TST) of the Qom Formation reflects relatively deeper microfacies. In the descriptions of this section, deepening trends are interpreted as

http://dx.doi.org/10.18268/BSGM2023v75n3a061023

a TST, shallowing trends are considered HST, and the fluctuation from deepening toward shallowing is referred to as the maximum flooding surface (MFS).

6.6.2.1 Depositional sequence 1

This sequence consists of TST and HST. The lower boundary of sequence 1 is correlated with the Red Formation. According to Figures 2, 9 and 10, it represents the type-1 sequence boundary (SB1) with evidence of subaerial exposure and concurrent subaerial erosion (iron oxide and limonite). This sequence boundary represents the SBZ 24 and is correlated with the global sequence boundary of Haq and Shutter (2008) and other studies (Figure 9). As a result of marine transgression, the TST is characterized by interaclast bioclastic wackestone, bioclastic miliolid packstone, and coral framestone microfacies.

In the following, MFS is characterized by bioclastic rudstone. Interaclast bioclastic wackestone indicates the deposition of the HST, while the upper part of the HST is interpreted by sandy mudstone representing the beginning of the marine regression. In sequence 1, the HST is characterized by interaclast bioclastic wackestone, bioclastic miliolid packstone, peloidal bioclastic grainstone and sandy mudstone.

Regarding the lack of evidence of subaerial exposure, the upper boundary of sequence 1 is considered a type-2 sequence boundary (SB2). The first sequence in the study area decreases in thickness to the east. This sequence has the age of Aquitanian (SBZ 24). Therefore, it has not been observed by Amirshahkarami and Karevan (2015). It can be observed in the other correlated sections.

6.6.2.2 Depositional sequence 2

This sequence consists of TST and HST. In sequence 2, the TST starts with ooidal grainstone and is composed of coral framestone, peloidal bioclastic grainstone, bioclastic wackestone, and bioclastic rudstone. Bioclastic rudstone microfacies show rising sea levels, reaching a maximum equal to MFS (Figures 2 and 9). The HST starts with peloidal bioclastic grainstone and consists of sandy bioclastic mudstone, interaclast bioclastic wackestone, and bioclastic miliolid packstone and shows marine regression.

The sequence boundary between DS1 and DS2 is characterized by abrupt microfacies shift from middle to outer shelf microfacies, without any evidences of subaerial exposure. This sequence boundary represent the SBZ24 and is correlated with the global sequence boundary of Haq and Shutter (2008). This Aquitanian age sequence is observed in three correlated sections (Figure 9). In addition, this sequence can be separated from other sequences by increasing the fossil debris and has an exclusive thickness.

6.6.2.3 Depositional sequence 3

Sequence 3 is in accord with the Burdigalian in age (SBZ25) and consists of TST and HST. The TST is characterized by open marine and barrier microfacies. The bioclastic rudstone with brachiopods and bryozoans shows the mfs. Marine regression begins with ooidal grainstone and comprises bioclastic mudstone, interaclast bioclastic wackestone, and bioclastic miliolid packstone.

The sequence boundary between DS3 and DS4 is characterized by abrupt microfacies shift from middle to outer shelf microfacies, without any evidence of subaerial exposure (Figures 2 and 9). This sequence includes calcareous sand and it suggests a decrease in depth from east to west. This third-order sequence consists of a series of progressive and retrograde small cycles. It is notable that the sequence can be separated by decreasing depth.

6.6.2.4 Depositional sequence 4

The depositional sequence 4 includes a deepening part mainly formed by middle and outer shelf microfacies. The deepening part of DS4 is defined by a retrogradational stacking pattern with the

http://dx.doi.org/10.18268/BSGM2023v75n3a061023

margin of grainstone-rudstone and open marine microfacies. The MFS is located in the lower part of outer shelf microfacies. This sequence is also Burdigalian in age (SBZ25) and consists of TST and HST. In the sequence 4, the TST is characterized by the barrier and open marine microfacies, starting with boundstone microfacies and ending with bioclastic rudstone microfacies.

Bioclastic rudstone microfacies show the maximum equivalent to MFS (Figures 2 and 9).

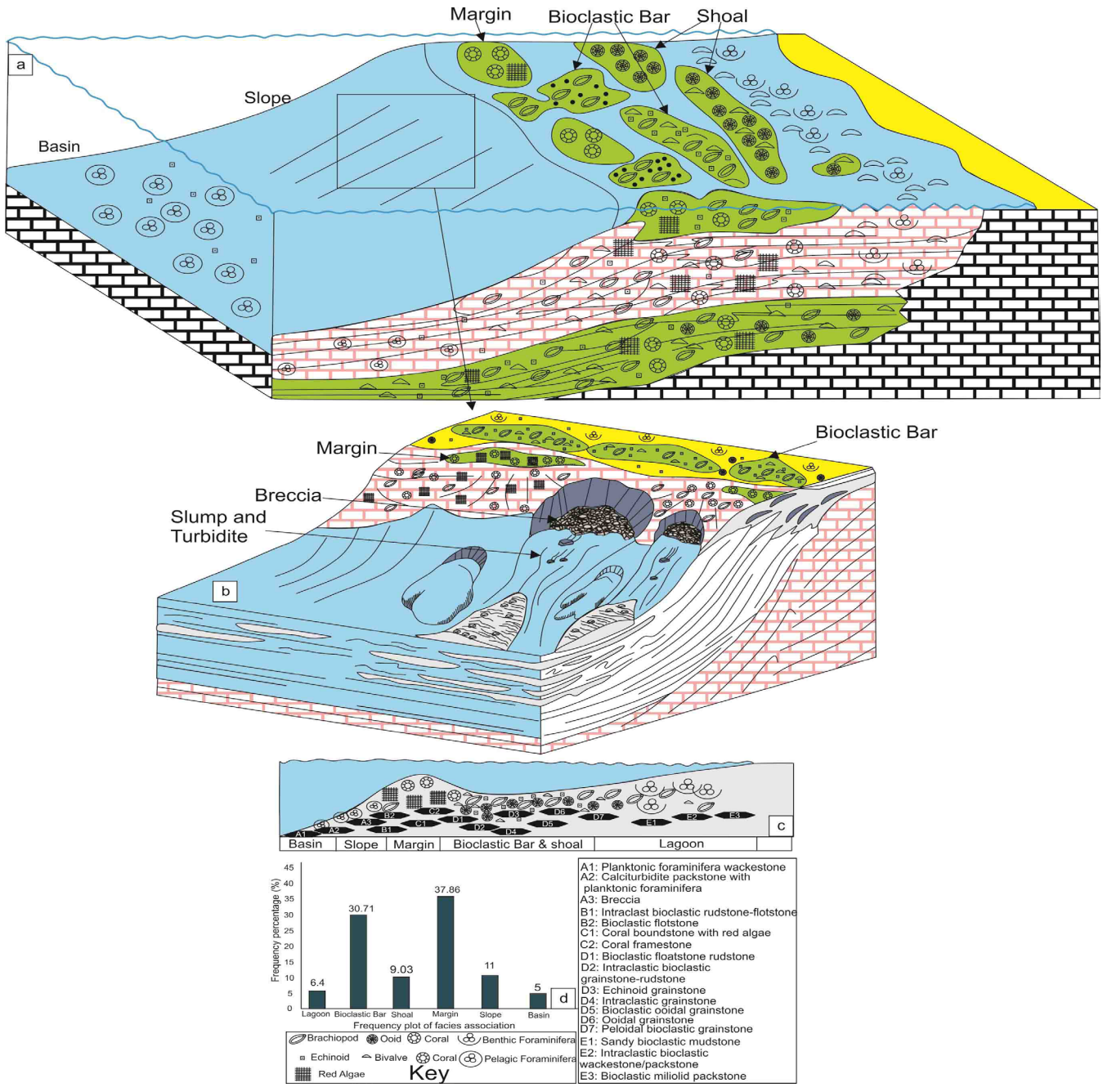

Figure 8 **Sedimentary model of the Qom Formation: a) Distribution of the facies associations (FAs) in a Shelf model; b) The architecture of the slope; c) The placement and distribution of microfacies on the two-dimensional model of the carbonate shelf; and d) Column chart showing the abundance of microfacies in different facies associations.**

http://dx.doi.org/10.18268/BSGM2023v75n3a061023

The HST is characterized by barrier and lagoon microfacies, suggesting the start of the marine regression. The upper boundary of this sequence is type 2. In the sequence 4 there is the LST system tract. This LST starts with ferruginous sandy limestone (Ghalibaf section) and limestone (Figure 9). The beginning of fossiliferous calcareous sandstone with fossil debris in all sections shows the transgressive surface (TS) and the beginning of TST. The MFS of sequence 4 is identified by bioclastic rudstone microfacies. Debris fossils in shale are most likely due to the shelf conditions during the maximum transgression. The HST of this sequence is dominated by limestone and shallow open marine toward-shore microfacies. The early HST of the studied section is characterized by a proliferation of shoal microfacies and grain-supported lagoon (e.g., small fossils, peloid, ooid, and grain quartz).

6.6.2.5 Depositional sequence 5

The sequence is Burdigalian in age (SBZ25) and composed of TST and HST. The TST is characterized by the lagoon, barrier, and open marine microfacies, in the order of their appearance. The MFS is characterized by bioclastic packstone microfacies. The HST consists of the barrier and lagoon microfacies, starting with bioclastic mudstone and interaclast bioclastic wackestone and ending with bioclastic miliolid packstone. In this sequence, the upper boundary is type 2 and correlated with the sequence proposed by Vail *et al.* (1984), and Galloway, (1989). This sequence has the highest thickness in the studied section.

The boundary between sequences 5 and 6 is associated with shoal toward lagoon microfacies. This boundary shows no clear evidence of the abrupt sea level decline. A sudden decline in sea level caused the formation of a composite sequence boundary at the base of the TST sediments (Figures 2 and 9). These deposits are interpreted as the early HST, primarily including shoal microfacies. The late HST shows an increasing trend towards sedimentation (shallow and lagoon microfacies), suggesting the filling of accommodation space. The SB type 2 is the upper boundary of the third depositional sequence at all sections. In these sections, increased sediment supply due to tidal flat (bird eye fabric) transgression is recorded by the deposition of TST marine sediments. This sequence is observed in Amirshahkarami and Karevan (2015) of the Burdigalian age (Figure 9).

6.6.2.6 Depositional sequence 6

This sequence is Burdigalian in age (SBZ25) and composed of TST and HST. In the sequence, the TST starts with bioclastic miliolid packstone microfacies of the lagoon environment, followed by the coral framestone and the microfacies of the open marine environment (bioclastic wackestone and bioclastic rudstone).

The HST is characterized by barrier microfacies and lagoon microfacies, including interaclast bioclastic wackestone and bioclastic miliolid packstone. The upper boundary of this sequence is considered in type 2 and correlated with the global sequence boundary of Haq and Shutter (2008). The aggradational depositional pattern is distinguished by a long period of marine conditions, indicating a balanced situation between sedimentation and accommodation (Bayet-Goll *et al.*, 2022). In the studied section, the gradual sea level rise generated the conditions for depositing thin packages of shallow-water sediment on a sub-horizontal depositional surface. At this sequence, the balance between accumulation and accommodation, led to an aggrading stacking pattern.

The MFS of this sequence is recognized by the largest landward retreat of bioclast fossils observed in a wackestone and packstone texture. This retreat occurs within deeper water microfacies corresponding to a relatively thin interval of scarce sedimentation (Figure 9). This level might be a marine flooding surface within the TST.

After the MFS, a normal regression trend is characterized by a prograding bioclastic shelf margin, leading to a reduction in accommodation space. Progradation of deposits might have

http://dx.doi.org/10.18268/BSGM2023v75n3a061023

occurred during the HST. During this event, the space between the buildups by mudstone and limestone was filled, where the deposits above the mounds were thin to absent.

6.6.2.7 DEPOSITIONAL SEQUENCE 7

The sequence is Burdigalian in age (SBZ25) and composed of TST and HST. The retrogradational package of the microfacies begins with lagoonal microfacies overlain by margin microfacies. The retrogradational stacking pattern culminated in deep marine marly limestone microfacies. The HST includes common shoaling–upward cycles, which consist of open marine and shoal bioclastic microfacies that are progradationally overlain by lagoonal microfacies.

The TST is characterized by coral framestone related to the barrier and bioclastic packstone, bioclastic wackestone, and bioclastic rudstone associated with an open-sea environment. The HST consists of ooidal grainstone related to the barrier

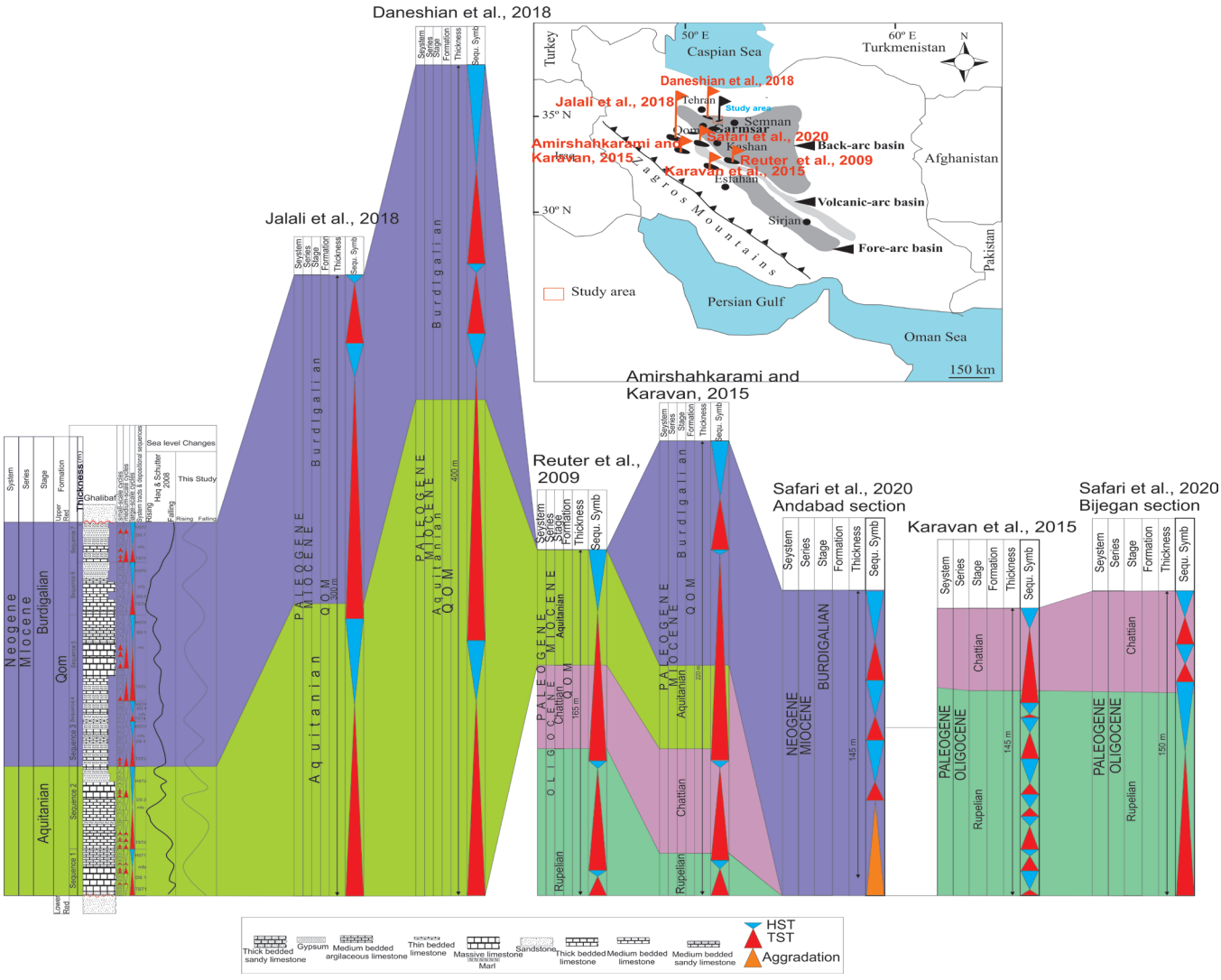

Figure 9 A measured stratigraphic section with the sedimentological characteristics and interpreted depositional environments and sequence stratigraphy of the Qom Formation between the study area and other sections in the Qom back-arc and volcanic arc basins which are comparable to the third-order sea level sequences by Haq and Schutter (2008).

http://dx.doi.org/10.18268/BSGM2023v75n3a061023

environment and sandy bioclastic mudstone, intraclast bioclastic wackestone, and bioclastic miliolid packstone of the lagoon environment.

The sequence's upper boundary is type 2 and is correlated with the global sequence of Haq and Shutter (2008). On the other hand, its lower boundary (TST) is identified by shoal microfacies with intercalated shale. The MFS is characterized by small foraminifera-rich marine microfacies separating HST from TST. It seems that the MFS is overlain by an intraclast bioclast with highly abundant debris fossils. These deposits are interpreted as the early HST, with their deposits mainly composed of shoal microfacies (Figure 10).

Interbedded shoal deposits with calcareous shale alternations evidenced the late HST

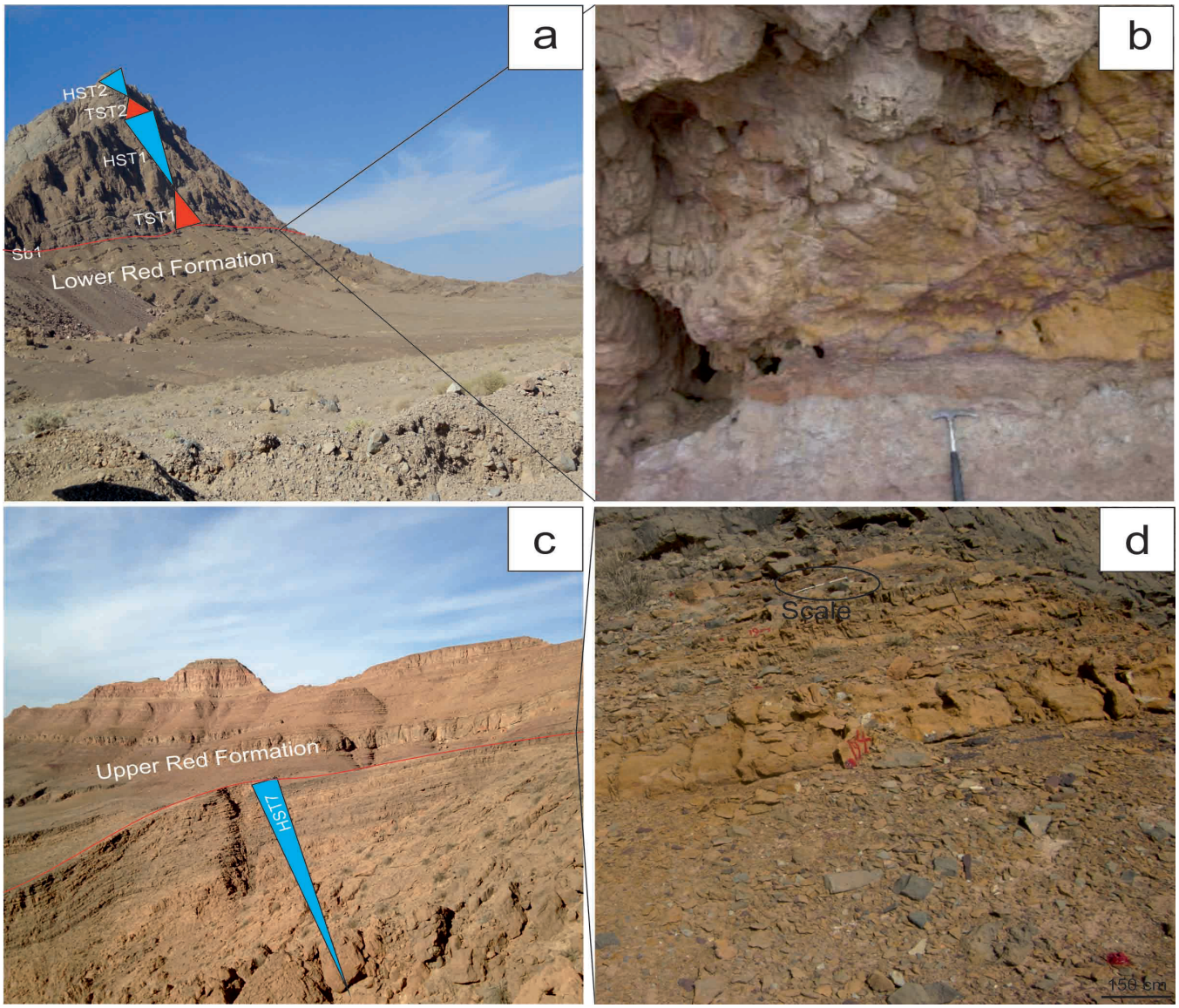

Figure 10 Field photographs of sequence boundaries in the Ghalibaf area: a) Field view of sequence boundary between Lower Red Formation and the Qom Formation, TST, and HST systems tract of the first and two depositional sequences; b) A close-up view of figure a with evidence of limonite and iron oxide between the Lower Red Formations and Qom Formation showing evidence of subaerial exposure and type-1 sequence boundary; c) Field photograph of HST systems tract of seven depositional sequences and sequence boundary between the Upper Red Formation and the Qom Formation, respectively; d) A close-up view of figure c with evidence of the boundary between the Qom Formation and Upper Red Formation.

http://dx.doi.org/10.18268/BSGM2023v75n3a061023

deposits. The late HST reveals an increasing sedimentation trend (shallow and shoal microfacies), suggesting an accommodation space filling. The above sequence is observed only in the section of this study and is not observed in other studies.

7. Conclusion

The Ghalibaf section has been studied for a better understanding of petrographic analysis, palaeoenvironmental conditions, sequence stratigraphy and biostratigraphy. Microfacies analysis recognized a carbonate platform developed on rimmed carbonate shelf with an effective barrier reef (reefal, oolitic and bioclastic barriers). They are grouped into five sedimentary environments including a lagoon, upper slope, lower slope, platform-margin sand shoals, and margin.

According to the foraminifera identified in the studied section, these deposits correspond to the Late Aquitanian-Burdigalian (SBZ24-SBZ25) timespan. Therefore, the Qom Formation in the Ghalibaf section has an estimated age of the Early Miocene. Based on microfacies analysis, seven third-order depositional sequences in the Ghalibaf area have been identified.

Comparing the global sea-level fluctuations with the relative sea-level changes which shows a significant correlation between the upper and lower sequence boundaries of the Qom Formation and the Aquitanian-Burdigalian boundary. Therefore, the differences in other sequence boundaries might be due to the effects of local tectonic activity in the Qom Formation sedimentary basin.

Contributions of authors

JS: investigation and writing original draft. YN: fieldwork and sampling, investigation, methodology, conceptualization, writing original and final/editing drafts. MP: investigation. STN: investigation, conceptualization. SS: investigation and writing/editing the final draft. MH: investigation, methodology, conceptualization, writing original and final/editing drafts.

Acknowledgements

Constructive suggestions to improve the manuscript by the referees are gratefully acknowledged. In addition, we would especially like to thank the editor, Prof. Francisco Vega.

Financing

There was no separate funding for this paper.

Conflict of interest

The authors declare no conflict of interest. Data availability statement. All thin sections are deposited in the Geology Section of the University of Gonabad. The datasets used in this work are already included within the article.

References

Abaie, I., Ansari, H.J., Badakhshan, A., Jaafari, A., 1964, History and development of the Alborz and Sarajeh fields of Central Iran: Bulletin of Iranian Petroleum Institute, 15, 561-574.

Adams. T., Bourgeois, F., 1967, Asmari biostratigraphy: Iranian Oil Operating Companies. Geological and Exploration Division, Report No. 1074.

Adams, C.G., Gentry, A.W., Whybrow, P.J., 1983, Dating the terminal Tethyan event: Utrecht Micropaleontological Bulletins, 30, 273–298.

Agard, P., Omrani, J., Jolivet, L., Mouthereau, F., 2005, Convergence history across Zagros (Iran): constraints from collisional and earlier deformation: International Journal of Earth Science, 94, 401-419. https://doi.org/10.1007/s00531-005-0481-4

Aghanabati, A., 2006, Geology of Iran: Geological Survey of Iran, Teheran, 560 p (In Persian).

Alavi, M., 1994, Tectonics of the Zagros orogenic belt of Iran: new data and interpretations: Tectonophysics, 229, 211–238. https://doi.org/10.1016/0040-1951(94)90030-2

Amirshahkarami, M., Karevan, M., 2015, Microfacies models and sequence stratigraphic architecture of the Oligocene-Miocene, Qom Formation, south of Qom, Iran: Geoscience Frontiers, 6, 593-604. http://dx.doi.org/10.1016/j.gsf.2014.08.004

Bachmann, M., Hirisch, F., 2006, Lower Cretaceous carbonate platform of the eastern Levant (Galilee and the Golan Heights), Stratigraphy and second order sea-level change: Cretaceous Research, 27, 478-512. http://dx.doi.org/10.1016/j.cretres.2005.09.003

Bayet-Goll, A., Sharafi, M., Daraei, M., Nasiri, Y., 2023, The influence of hybrid sediment gravity flows on distribution and composition of trace-fossil assemblages: Ordovician succession of the north-eastern Alborz Range of Iran: Sedimentology, 70, 783-827. https://doi.org/10.1111/sed.13058

Bayet-Goll, A., Daraei, M., Seginsara, M.I., 2022, Palaeogeographic reconstruction and sequence architecture of the middle-upper Jurassic successions of Hawraman Basin (NW Iran): Implications for tectono-depositional processes of the northeastern passive margin of the Arabian Plate: Geological Journal, 57(5), 2058 2093. https://doi.org/10.1002/gj.4407

Berberian, M., 2005, The 2003 Bam urban earthquake: a predictable seismotectonic pattern along the western margin of the rigid Lut block, southeast Iran: Earthq Spectra, 21, 35–99. https://doi.org/10.1193/1.2127909

Berberian, M., King, G.C.P., 1981, Towards a paleogeography and tectonic evolution of Iran. Canadian: Earth Science Review, 18, 210-265. https://doi.org/10.1139/e81-019

Bignot, G., Guernet, C., 1976, Sur la présence de Borelis curdica (Reichel) dans le Miocène de l'ile de Kos (Grèce): Géologie Méditerranéenne, 3 (1), 15-25. https://doi.org/10.3406/geolm.1976.959

Boukhary, M., Abdelghany, O., Hussein-Kamel, Y., Bahr, S., Alsayigh, A.R., Abdelraouf, M., 2010, Oligocene larger foraminifera from United Arab Emirates, Oman and Western Desert of Egypt: Historical Biology, 22, 348–366. https://doi.org/10.1080/08912960903570047

Bover-Arnal, T., Pascual-Cebrian, E., Skelton, P.W., Gili, E., Salas, R., 2015, Patterns in the distribution of Aptian rudists and corals within a sequence-stratigraphic framework (Maestrat Basin, E Spain): Sedimentary Geology, 321, 86–104. https://doi.org/10.1016/j.sedgeo.2015.03.008

Bozorgnia, F., 1965, Qum Formation stratigraphy of the Central Basin of Iran and its intercontinental position: Bulletin of the Iranian Petroleum Institute, 24, 69-75.

Brandano, M., Morsilli, M., Vannucci, G., Parente, M., Bosellini, F., Vicens, G., 2010, Rhodolith-rich lithofacies of the Porto Badisco Calcarenites (Upper Chattian, Salento, and Southern Italy): Italian Journal Geoscies, 1291, 119–131. https://doi.org/10.3301/IJG.2009.10

Cahuzac, B., Poignant, A., 1997, Essai de biozonation de l'Oligo-Miocène dans les bassins européens: à l'aide des grands foraminifères néritiques: Bulletin de la Société géologique de France, 168, 155-169.

Daneshian, J., Dana, L.R., 2007, Early Miocene benthic foraminifera and biostratigraphy of the Qom Formation, Deh Namak, central Iran: Journal of Asian Earth Sciences, 29, 844- 858. https://doi.org/10.1016/j.jseaes.2006.06.003

Della Porta, G., Kenter, J.A.M., Bahamonde, J.R., 2003, Depositional facies and stratal geometry of an Upper Carboniferous prograding and aggrading highrelief carbonate platform (Cantabrian Mountains, N Spain):

Sedimentology, 51, 267–295. https://doi.org/10.1046/j.1365-3091.2003.00621.x

Della Porta, G., Kenter, J.A.M., Bahamonde, J.R., Immenhauser, A., Villa, E., 2002, Microbial boundstone dominated carbonate slope (Upper Carboniferous, NSpain): microfacies, facies distribution stratal geometry: Facies, 49, 175–207. https://doi.org/10.1007/s10347-003-0031-0

Dunham, R.J., 1962: Classification of carbonate rocks according to depositional texture. In: Ham, W.E. (ed.), Classification of Carbonate Rocks - A Symposium. AAPG, 1, 108-121. https://doi.org/10.1306/M1357

Eberli, G.P., 1987, Calcareous Turbidites and their relationship to sea- level fluctuations and tectonism, in Einsele, G. Ricken, W. Seilacher, A. (Eds.), Cycles and Events in Stratigraphy: Springer, Verlag, 33, 340-359. https://doi.org/10.1016/S0037-0738(97)00044-4

Embry, A.F., Klovan, E.J., 1971, Absolute water limits of the Devonian paleoecological zones: Geologische Rundschau, 61, 2. https://doi.org/10.1007/BF01896340

Fagerstrom, J.A., 1991, Reef-building guilds and a checklist for determining guild membership: Coral Reefs, 10, 47-52. https://doi.org/10.1007/BF00301908

Flügel, E., 2010, Microfacies of Carbonate Rocks, Analysis Interpretation and Application: Springer-Verlag, New York, 976 p. https://doi.org/10.1007/978-3-642-03796-2

Fournier, F., Montaggioni, L., Borgomano, J., 2004, Paleoenvironments and high-frequency cyclicity from Cenozoic South-East Asian shallow-water carbonates: a case study from the Oligo-Miocene buildups of Malampaya, Offshore Palawan, Philippines: Marine and Petroleum Geology, 21, 1-21. https://doi.org/10.1016/j.marpetgeo.2003.11.012

Furrer, M.A., Soder, P.A., 1955, The Oligo-Miocene marine formation in the Qum region (Central Iran). Rome, Italy, In Proceedings of the 4th World Petroleum Congress, Rome, 267-277. Section I/A/5.

Fürsich, F., Pandey, D. K., 2003, Sequence stratigraphic significance of sedimentary cycles and shell concentrations in the Upper Jurassic–Lower Cretaceous of Kachchh, western India: Palaeogeography, Palaeoclimatology, Palaeoecology, 193(2), 285-309. https://doi.org/10.1016/S0031-0182(03)00233-5

Galloway, W.E., 1989, Genetic Stratigraphic Sequences in Basin Analysis I: Architecture and Genesis of Flooding-Surface Bounded Depositional Units: AAPG Bulletin, 73, 125-142. https://doi.org/10.1306/703C9AF5-1707-11D7-8645000102C1865D

Geel, T., 2000, Recognition of stratigraphic sequences in carbonate platform and slope deposits: empirical models based on microfacies analysis of Paleogene deposits in southeastern Spain: Palaeogeography, Palaeoclimatology, Palaeoecology, 155, 211-238. https://doi.org/10.1016/S0031-0182(99)00117-0

Haas, J., Götz. A.E., Pálfy, J., 2010, Late Triassic to Early Jurassic palaeogeography and eustatic history in the NW Tethyan realm: New insights from sedimentary and organic facies of the Csővör Basin (Hungary): Palaeogeography, Palaeoclimatology, Palaeoecology, 291, 456–468. https://doi.org/10.1016/j.palaeo.2010.03.014

Hadi, M., Forouzande, S. K., Consorti, L., Parandavar, M., Vahidinia, M., 2023, Extending the stratigraphic range of Nummulites bormidiensis Tellini in the Neo-Tethys (Zagros basin, SE Iran) through biometry and calcareous nannofossil biostratigraphy: Micropaleontology, 69(4), 515-532. https://doi.org/10.47894/mpal.69.4.06

Haq, B.U., Shutter, S.R., 2008, A chronology of Paleozoic sea level changes: Science, 322, 64-68. https://doi.org/10.1126/science.1161648

Harzhauser, M., Piller, W.E., 2007, Benchmark data of a changing sea—palaeogeography, palaeobiogeography and events in the Central Paratethys during the Miocene: Palaeogeography, Palaeoclimatology, Palaeoecology, 253(1-2), 8-31. https://doi.

org/10.1016/j.palaeo.2007.03.031

Henson, F.R.S., 1948, Larger imperforate Foraminifera of Southwestern Asia: Families Lituolidue, Orbitolinidae and Meandropsinidae: British Museum Natural History, pp 1–127. Bib ID: 2400676.

Hottinger, L., 2007, Revision of the foraminiferal genus Globoreticulina Rahaghi, 1978, and of its associated fauna of larger foraminifera from the Late Middle Eocene of Iran: Carnets de Géologie, Series CG, 106, 1-51. https://doi.org/10.4267/2042/9213

James, G., Wynd, J., 1965, Stratigraphic nomenclature of Iranian oil consortium agreement area: AAPG Bulletin., 49, 2182-2245. https://doi.org/10.1306/A663388A-16C0-11D7-8645000102C1865D

Kenter, J.A.M., Ginsburg, R.N., Troelstra, S.R., 2001, Sea-level driven sedimentation patterns on the slope margin, in Ginsburg R.N., editor: Subsurface geology of a prograding carbonate platform margin, Great Bahama Bank: results of the Bahamas drilling project: Special Publication-SEPM, 70, 61-100. https://doi.org/ 10.2110/pec.01.70.0061

Kenter, J.A.M., Harris, P.M., Della Porta, G., 2005, Steep microbial boundstone dominated platform margins-examples implica- tions: Sedimentary Geology, 178, 5– 30. https://doi.org/10.1016/j.sedgeo.2004.12.033

Kikichi, K., Naruse, H., Kotake, N., 2018, Evaluation of ichnodiversity by image-resampling method to correct outcrop exposure bias: Palaios, 33(5), 204-217. https://doi.org/10.2110/palo.2017.090

Laursen, G.V., Monibi, S., Allan, T.L., Pickard, N.A., Hosseiney, A., Vincent, B., Hamon, Y., Van-Buchem, F.S.P., Moallemi, A., Druillion, G., 2009, The Asmari Formation revisited: changed stratigraphic allocation and new biozonation: First International Petroleum Conference & Exhibition, Shiraz, 1-5. http://dx.doi.org/10.3997/2214-4609.20145919

Li, M., Song, H.J., Tian, L., Woods, A.D., Dai, X., Song, H.Y., 2018, Lower Triassic deep sea carbonate precipitates from South Tibet, China: Sedimentary Geology, 376, 60-71. https://doi.org/10.1016/j.sedgeo.2018.08.004

Loeblich, A.R., Tappan, H., 1987, Foraminiferal Genera and Their Classification: New York, Van Nostrand Reinhold Company, 970 p. https://doi.org/10.1007/978-1-4899-5760-3.

Mohammadi, E., 2022, Foraminiferal biozonation, biostratigraphy and trans-basinal correlation of the Oligo-Miocene Qom Formation, Iran (northeastern margin of the Tethyan Seaway): Palaeoword. doi.org/10.1016/j.palwor.2022.04.005.

Mohammadi, E., Vaziri, M.R., Dastanpour, M., 2015, Biostratigraphy of the nummulitids and lepidocyclinids bearing Qom Formation based on larger benthic foraminifera (Sanandaj-Sirjan fore-arc basin and Central Iran back-arc basin, Iran): Arabian Journal Geoscience, 8, 403-423. https://doi.org/10.1007/s12517-013-1136-6

Morley, C.K., Kongwung, B., Julapour, A.A., Abdolghafourian, M., Hajian, M., Waples, D., Warren, J., Otterdoom, H., Srisuriyon, K., Kazemi, H., 2009, Structural development of a major late Cenozoic basin and transpressional belt in central Iran: the Central Basin in the Qom-Saveh area: Geosphere, 5, 325–362. https://doi.org/10.1130/GES00223.1

Mutti, E., Tinterri, R., Benevelli, G., Di Biase, D., Cavanna, G., 2003, Deltaic, mixed and turbidite sedimentation of ancient foreland basins: Marine and Petroleum Geology, 20, 733–755. https://doi.org/10.1016/j.marpetgeo.2003.09.001

Nabavi., 1974, Geological map of Semnan, scale 1/250000, Iran.

Nasiri, Y., Bayet-Goll, A., Mahboubi, A., Moussavi-Harami, R., Monaco, P., 2020, Paleoenvironmental control on trace fossils across a Mississippian carbonate ramp succession, Mobarak Formation, east of

http://dx.doi.org/10.18268/BSGM2023v75n3a061023

Central and Eastern Alborz, Iran: African Earth Sciences, 165, 103800. https://doi.org/10.1016/j.jafrearsci.2020.103800.

Özcan, E., Less, G., Báldi-Beke, M., Kollányi, K., 2010, Oligocene hyaline larger foraminifera from Kelereşdere Section (Muş, Eastern Turkey): Micropaleontology, 56, 465–493. https://doi.org/ 10.47894/mpal.56.5.04

Pedley, M., 1998, A review of sediment distributions and processes in Oligo–Miocene ramps of southern Italy and Malta (Mediterranean divide): Journal of the Geological Society of London, Special Publications, 149, 163–179. https://doi.org/10.1144/GSL.SP.1999.149.01.09

Reichel, A., 1936-1937, Etude sur les Alvéolines: Mémoires de la Société Paleontologique Suiss, LVII-LIX , 1-147.

Reuter, M., Piller, W.E., Harzhauser, M., Mandic, O., Berning, B., Rögl, F., Kroh, A., Aubry, M.P., Wielandt-Schuster, U., Hamedani, A., 2009, The Oligo-/Miocene Qom Formation (Iran): evidence for an early Burdigalian restriction of the Tethyan Seaway and closure of its Iranian gateways: International Journal of Earth Science, 98, 627–650. https://doi.org/10.1007/s00531-007-0269-9

Saraswati, P.K., Khanolkar, S., Banerjee, S., 2018, Paleogene stratigraphy of Kutch, India: an update about progress in foraminiferal biostratigraphy: Geodinamica Acta, 30, 100–118. https://doi.org/10.1080/09853111.2017.1408263

Schuster, F., Wielandt, U., 1999, Oligocene and Early Miocene coral faunas from Iran: palaeoecology and palaeobiogeography: International Journal of Earth Sciences, 88, 571-581. https://doi.org/10.1007/s005310050285

Sirel, E., 2003, Foraminiferal description and biostratigraphy of the Bartonian, Priabonian and Oligocene shallow-water sediments of the southern and eastern Turkey: Revue de Paleobiologie, 22(1), 269-339.

Sirel, E., Acar, Ş., 1982, *Praebullalveolina*, a new foraminiferal genus from the upper Eocene Afyon and Çanakkale regions (W of Turkey): Eclogae Geologicae Helvetiae, 75(3): 821-839.

Sirel, E., Ozgen Erdem, N., Kangal, O., 2013, Systematics and biostratigraphy of Oligocene (Rupelian-Early Chattian) foraminifera from lagoonal-very shallow water limestone in the eastern Sivas Basin (central Turkey): Geologia Croatica, 66(2), 83-110. https://doi.org/10.4154/GC.2013.07

Sirel, E., Özgen-Erdem, N.: Sinanoglu, D., 2020, Foraminiferal Description of the Miocene Shallow-Water Limestone from the Diyarbakır and Siirt Areas of Southeast Turkey: Journal of the Palaeontological Society of India, 65(2), 31.

Soder, P.A., 1959, Detailed investigations on the marine formation (Oligo-Miocene) of Qum. Exploration Directorate of NIOC, Geological report No. 186, 54P.

Stöcklin, J. 1968, Structural history and tectonics of Iran, A review: American Association of Petroleum Geologists Bulletin, 52, 1229–1258. https://doi.org/10.1306/5D25C4A5-16C1-11D7-8645000102C1865D

Stöcklin, J., Setudehnia, A., 1991, Stratigraphic Lexicon of Iran: Geological Survey of Iran, Report No. 18, 40-41.

Taghdisi Nikbakht, S., Rezaee, P., Mousavi-Harami, R., Khanehbed, M., Ghaemi, F., 2019, Facies Analysis, Sedimentary Environment and Sequence stratigraphy of Khan Formation in Kalmard Area, Central Iran: Implications for Lower Permian Palaeogeography: Neues Jahrbuch für Geologie und Paläontologie, 292(2), 129-154. https://doi.org/10.1127/njgpa/2019/0812

Tucker, M.E., 1985, Shallow marine carbonate facies and facies models, in Brenchley, P.J. Williams B.P.J. (eds.), Sedimentology, recent development and applied aspects: Journal of the Geological Society of London, Special

Publications, 18, 139-161. https://doi.org/10.1144/GSL.SP.1985.018.01.08

Tucker, M.E., Wright, V.P., 1990, Carbonate Sedimentology: Blackwell Science Publication Oxford, 425 p.

Vail, P.R., Hardenbol, J., Todd, RG., 1984, Jurassic unconformities, chronostratigraphy and sea level changes from seismic stratigraphy, in Schlee, J.S. (ed.) Interregional unconformities and hydrocarbon exploration: American Association of Petroleum Geologists Memoir, 33, 129–144.

Van Buchem, F.S.P., Allan, T.L., Laursen, G.V., Lotfpour, M., Moallemi, A., Monibi, S., Motiei, H., Pickard, A.R., Tahmasbi, N.A.H., Vedrenne, V., Vincent, B., 2010, Regional stratigraphic architecture and reservoir types of the Oligo-Miocene deposits in the Dezful Embayment (Asmari and Pabdeh Formations) SW Iran: Journal of the Geological Society of London, Special Publications, 329, 219-263. https://doi.org/10.1144/SP329.10

Vaziri-Moghaddam, H., Kimiagari, M., Taheri, A., 2006, Depositional environment and sequence stratigraphy of the Oligo-Miocene Asmari Formation in SW Iran: Facies, 52, 41–51. https://doi.org/10.1007/s10347-005-0018-0

Warren, W.J., 2000, Dolomite: Occurrence, evolution and economically important association: Earth science review, 52, 1-81. https://doi.org/ 10.1016/S0012-8252(00)00022-2

Wilson, J.L., 1975, Carbonate Facies in Geological History: Springer Verlag, New York, 471 p. https://doi.org/10.1007/978-1-4612-6383-8

Yazdi Moghadam, M., Sarfi, M., Ghasemi Nejad, E., Sadeghi, A., Sharifi, M., 2021, Early Miocene larger benthic foraminifera from the northwestern Tethyan Seaway (NW Iran): new findings on Shallow Benthic Zone 25: International Journal of Earth Sciences, 110, 719-740. https://doi.org/10.1007/s00531-021-01986-1

Yazdi-Moghadam, M., Sadeghi, A., Adabi, M.H., Tahmasbi A.R., 2018a, Foraminiferal biostratigraphyof the lower MioceneHamzian and Arashtanab sections (NW Iran) northern margin of the Tethyan: Geobios, 51, 211-246. https://doi.org/ 10.1016/j.geobios.2018.04.008

Yazdi-Moghadam, M., Sadeghi, A., Adabi, M.H., Tahmasbi, A., 2018b, Stratigraphy of the Lower Oligocene nummulitic limestones, north of Sonqor (NW Iran): Rivista Italiana di Paleontologia e Stratigrafia, 124, 407–419. https://doi.org/10.13130/2039-4942/10271